Received: 12 June 2020 | Revised: 30 March 2021 | Accepted: 14 April 2021

DOI: 10.1002/joc.7142

RESEARCH ARTICLE

International Journal of Climatology RMetS

# Evaluation of multiple reanalyses in reproducing the spatio-temporal variability of temperature and precipitation indices over southern South America

**Rocio Balmaceda-Huarte**[1,2,3] | **Matias Ezequiel Olmo**[1,2,3] | **Maria Laura Bettolli**[1,2,3] | **Maria Mercedes Poggi**[1,4]

[1]Department of Atmospheric and Ocean Sciences, Faculty of Exact and Natural Sciences, University of Buenos Aires (DCAO-FCEN-UBA), Buenos Aires, Argentina

[2]National Council of Scientific and Technical Research (CONICET), Buenos Aires, Argentina

[3]Institut Franco-Argentin d'Estudes sur le Climat et ses Impacts, Unité Mixte Internationale (UMI-IFAECI/CNRS-CONICET-UBA), Buenos Aires, Argentina

[4]Department of Climatology, National Weather Service of Argentina (SMN), Buenos Aires, Argentina

**Correspondence**
Rocio Balmaceda-Huarte, Faculty of Exact and Natural Sciences, University of Buenos Aires, Intendente Güiraldes 2160, Ciudad Universitaria, Buenos Aires City, C1428EGA Buenos Aires, Argentina.
Email: rbalmaceda@at.fcen.uba.ar

**Funding information**
Agencia Nacional de Promoción Científica y Tecnológica, Grant/Award Number: PICT-2018-02496; Universidad de Buenos Aires, Grant/Award Numbers: 20020170100357BA, 2018-20020170100117BA

## Abstract

Several temperature and precipitation indices, with special focus on extremes, were analysed in different sub-regions of southern South America during 1979–2017 using multiple reanalyses, the CPC gridded data set and the most extended network of meteorological stations employed in regional climate studies up to date. Reanalyses generally well represented the spatial patterns of the indices, although they showed some differences in extreme indices over large portions of southern South America and tended to overestimate precipitation maximums, especially in southern Chile. Furthermore, ERA-Interim presented clear difficulties in reproducing precipitation near the Andes Mountains, exhibiting the largest overestimations. This seemed to be improved in the new generation of ERA reanalyses (ERA5). When evaluating the long-term changes, most of the data sets agreed in general warming conditions, stronger and more homogeneous for the maximum temperature. NCEP1 and NCEP2 reanalyses showed contrary temporal changes in almost all the temperature indices. Precipitation indices exhibited less consistent changes among reanalyses, although significant upward trends were detected for precipitation extremes in southeastern South America and downward trends were detected in southern Chile in the observational data sets. In addition, most of the data sets agreed in drier conditions in the arid diagonal region of Argentina as reflected by significant positive trends for dry spells and negative trends for the total annual precipitation. In terms of the inter-annual correspondence, reanalyses usually presented good correlations to the stations reference in the regional averaged series, mainly for temperature indices and more variable for precipitation indices. Overall, no reanalysis was found to perform best. The use of reanalyses data to perform regional climate studies should consider the existent differences among them and with observational data. Moreover, using multiple sources of information is strongly recommended to account for observational uncertainty, especially in regions like southern South America, where data availability and its resolution are often limited.

  

KEYWORDS
extreme climate indices, observational uncertainty, reanalysis, southern South America, trends

## 1 | INTRODUCTION

Southern South America (SSA) (roughly between 22–57°S and 49–74°W) is an extended region that presents a wide variety of climates and has been characterized by a changing climate (Saurral *et al*., 2016; de Barros Soares *et al*., 2017; Burger *et al*., 2018). Temperature and precipitation indices are useful tools for monitoring when changes in climate occur and have been commonly used for the evaluation of climate change around the world and also in SSA (Marengo *et al*., 2010; Skansi *et al*., 2013; Donat *et al*., 2016; Lovino *et al*., 2018). Although trends highly depend on the region, general warming signals have been documented over SSA, whereas region-dependent drying and wetting signals have been recorded, with significant increases particularly in extremes (Re and Barros, 2009; Quintana and Aceituno, 2012; Vicuña *et al*., 2013; Rusticucci *et al*., 2016; Olmo *et al*., 2020).

The study of climate variability and the understanding of global and regional climate change is strongly linked to the available information over a region. Particularly, observations from meteorological stations play a critical role in performing climate studies. However, their temporal and spatial coverage strongly depends on the region. In-situ observations in SSA are not always spatially and temporally sufficient, and they often have gaps in their temporal series and errors that need to be evaluated before performing any climate study, evaluation or model validation over the region. It is therefore that other state-of-the-art products are commonly employed in these procedures, such as gridded data sets from multiple sources, satellite data and reanalyses. Nevertheless, it is important to understand their advantages and limitations.

Reanalysis-based products are currently some of the most used data sets, providing global information over long time periods of the different levels of the atmosphere at regular intervals, which make them convenient for the evaluation of climate models, for attribution studies and further purposes. These data sets are produced by data assimilation, based on both observations and model-based forecasts (Parker, 2016). The typical reanalysis data sets include surface and upper-air direct observations and also satellite products in the data assimilation system. The assimilated meteorological variables include temperature, pressure and wind speed, but not precipitation, which is estimated according to model physics and parameterizations (Maraun and Widmann, 2018). Generally, the assimilated variables can be expected to be very close to reality, whereas not-assimilated variables such as precipitation may present substantial biases (Widmann and Bretherton, 2000). The density of observed data are key in this regard, that is, the disagreement between two distinct reanalysis data sets is strongly linked to observational coverage (Sterl, 2004).

Moreover, reanalyses are frequently used as input sources for the assessment of the past and present climate, in the construction of different observational data sets and in the assessment of the added value in regional climate modelling (Weedon *et al*., 2014; Sun *et al*., 2018; Falco *et al*., 2019; Gutiérrez *et al*., 2019). Hence, these products need to be evaluated against observations before being implemented into various applications (Wang *et al*., 2019).

Reanalyses performance in reproducing surface variables has been widely evaluated in several studies (e.g., Donat *et al*., 2014; Lindsay *et al*., 2014; Isotta *et al*., 2015; Yang and Zhang, 2018; Wang *et al*., 2019; Krauskopf and Huth, 2020; Sheridan *et al*., 2020). Jones *et al*. (2013) pointed out that reanalysis products often fail in reproducing precipitation, especially at a daily time scale. Even more, they have a larger degree of variability than other types of precipitation data sets (Sun *et al*., 2018). For surface temperature, Luo *et al*. (2019) identified cold biases in complex terrain areas, correlated with the differences in elevation between the stations observations and the reanalysis models. In East Africa, Schmocker *et al*. (2016) compared station data with reanalyses and found that some products well reproduced the rainfall climatology and some the spatial trend pattern, but no product reproduced both. Over SSA, few studies have compared their performance against in-situ observations. Rusticucci and Kousky (2002) compared the NCEP/NCAR reanalysis versus information from about 20 stations during 1958–1998 for minimum and maximum temperature. The authors found good agreement over the low-elevation regions in central and eastern Argentina and poorer correspondence in the vicinity of the Andes mountains. Also using NCEP/NCAR, Dufek *et al*. (2008) analysed precipitation and temperature climate indices in several portions of South America and detected some regional differences in their trends when compared with gridded observational data, mainly for precipitation indices in northern Argentina. Furthermore, Rusticucci *et al*. (2014) found good skills and some

limitations of the ERA-Interim reanalysis performance on regional winter climate in the southern-central Andes, in comparison with gridded products containing in situ observations. Schumacher *et al.* (2020) compared ERA-Interim and MERRA2 reanalyses against in situ observations in reproducing precipitation and temperature in the Chilean Andes and detected larger mismatches in northern and southern portions of Chile for precipitation, whereas higher disagreement was observed for temperature in central Chile. However, intercomparison studies among different reanalyses in SSA are more limited. In a global study, Donat *et al.* (2014) analysed changes in climate extremes considering gridded observations and several reanalyses and found differences in the patterns of change in South America and pointed out the need for high-quality observational data in the region. Thus, evaluating reanalyses ability to perform regional climate studies is still not a fully addressed task in SSA. Therefore, providing a reference about uncertainties between observational data and reanalyses is of key importance for the region.

In this context, the main objective of this study is to evaluate the performance of several reanalysis data sets in reproducing the spatial and temporal variability (including trends) of temperature and precipitation indices in southern South America during the recent period. This assessment was carried out using in-situ and gridded observations to account for the observational uncertainty across the region. In this work, we set up the most extended data set of meteorological stations used for regional climate studies over southern South America up to date, with a fine balance between the spatial and temporal coverage of stations measuring both daily extreme temperatures and accumulated precipitation. The reanalysis and observational databases are described in Section 2, while Section 3 shows the performance results and Section 4 presents a discussion of them and final conclusions.

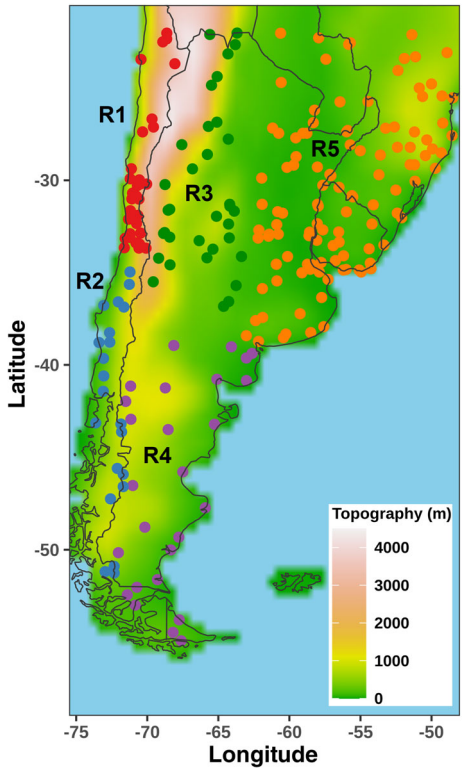


**FIGURE 1** Meteorological stations used over SSA during the period 1979–2017, sub-regionalized by colours and numbered R1 to R5. Shaded colours indicate SSA elevation (from the ERA-Interim reanalysis) expressed in meters [Colour figure can be viewed at wileyonlinelibrary.com]

## 2 | DATA AND METHODOLOGY

### 2.1 | Data

Daily accumulated precipitation, minimum and maximum temperature (TN and TX, respectively) observed at meteorological stations over SSA were considered during the period 1979–2017 (Figure 1). Data were provided by the National Weather Services of Argentina, Brazil, Paraguay and Uruguay, the National Institute of Agricultural Technology and the National Water Institute of Argentina and the Center for Climate and Resilience Research of Chile. Most of the meteorological stations used in this study presented less than 5% of missing data during the period of study for each of the three variables. Only a few stations located in southern Brazil with missing data up to 20% were considered for the analysis to guarantee spatial coverage.

A quality control was performed for each selected station based on the recommendations of Penalba and Vargas (2004) and Rusticucci and Barrucand (2001) for the region considering, among other aspects, the completeness of the station records, the evaluation of possible outliers in their time series (which were evaluated individually and compared with information from nearby stations) and the consistency of daily extreme temperatures (TX > TN). In those cases, the daily values were removed. Figure 1 shows the location of the 232 meteorological stations considered around SSA. Of all stations, 111 belong to Argentina, 56 to Chile, 38 to Brazil, 20 to Uruguay and 7 to Paraguay. The list of meteorological stations used in this study with the web pages of the data sources and the information about the data available to download were included in Table S1. Most of these stations were employed by the research group in previous studies (Olmo *et al.*, 2020). Despite the lack of stations with long records in some particular areas, the distribution

**TABLE 1** Specifications of the reanalysis used in this study during the period 1979–2017

| Data set | Labels | Horizontal resolution | Center | Reference |
|---|---|---|---|---|
| **ERA-Interim** | ERA.INTERIM | ∼0.75° | European Center for Medium-Range Weather Forecast (ECMWF) | Dee *et al*., 2011 |
| **ERA-5** | ERA5 | ∼0.25° | | Hersbach and Dee, 2016 |
| **JRA-55** | JRA55 | ∼0.56° | Japan meteorological agency (JMA) | Kobayashi *et al*., 2015 |
| **NCEP-R1** | NCEP1 | 1.875° | National Center for environmental prediction and National Center for Atmospheric Research (NCEP/NCAR) | Kalnay *et al*., 1996, Kistler *et al*., 2001 |
| **NCEP-R2** | NCEP2 | 1.875° | | Kanamitsu *et al*., 2002 |

of station points is relatively homogeneous. This database resulted in the most extended network of meteorological stations implemented in regional climate studies over SSA up to date. Note that, although other stations are available over some parts of the region, records of such in situ observations are not long enough to perform a trend analysis and many of them do not encompass the three variables of interest (daily precipitation, TN and TX).

Addressing climate studies of spatial and temporal variability require long records of high-quality observational data sets. This kind of studies should also consider different sources of information for the sake of a comprehensive spatio-temporal characterization and to account for observational uncertainty as well. This is particularly important for regions like SSA, where data availability is often limited. In this regard, the CPC Global Unified Gauge-based analysis of daily precipitation and CPC Global and CPC global daily temperature data sets from the NOAA Climate Prediction Center (Xie *et al*., 2007) were also considered during the period 1979–2017 for the analysis (available at https://psl.noaa.gov/data/gridded/). It is important to highlight that this is one of the few observational gridded data sets available at a daily scale for SSA at 0.5° × 0.5° grid resolution that includes the three variables of interest (daily precipitation, TN and TX).

The different reanalyses used at a daily scale are listed in Table 1. A brief description of these data sets are included below:

- ERA-Interim is a global reanalysis produced by the European Center for Medium-Range Weather Forecasts (ECMWF) initiated in 1979 (Dee *et al*., 2011). This data set is carried out with a 4D-Var data assimilation system with a 12 hr analysis window, making more complete use of observations collected between analysis times than in previous reanalyses from the ECMWF (Fujiwara *et al*., 2017). The horizontal resolution of the data set is near to 79 km (TL255 spectral grid) on 60 vertical levels up to 0.1 hPa;
- ERA-5 is the fifth generation reanalysis from ECMWF (Hersbach and Dee, 2016) at ∼0.25° spatial resolution, providing several improvements compared with ERA-Interim such as better representation of tropospheric processes, better global balance of precipitation and evaporation and more consistent sea surface temperatures and sea ice content (Hersbach and Dee, 2016; Hoffman et al., 2019). The analysis is produced with a 1 hr time step, using a significantly more advanced 4D-Var assimilation scheme. Data are provided on 137 vertical levels up to 0.01 hPa. In contrast to ERA-Interim, ERA5 includes a lower-resolution 10-member ensemble of data assimilations that brings additional information on the uncertainties in the reanalysis and their spatio-temporal changes (Hoffmann *et al*., 2019);
- JRA-55 (Kobayashi *et al*., 2015) is a global reanalysis product with a spatial resolution of ∼0.56° created by the Japan Meteorological Agency (JMA) released in 2013. JRA-55 uses a 4D-VAR with variational bias correction for satellite radiances (Wang *et al*., 2019). This data set has a resolution of about 55 km (TL319) and, in addition to the surface level, includes other 60 more levels up to 0.1 hPa;
- NCEP-R1 (Kalnay *et al*., 1996; Kistler *et al*., 2001)—first released in 1995—is produced by the National Centers for Environmental Prediction and National Center for Atmospheric Research system with extended temporal coverage from 1948. It is generated using a modified version of the NCEP forecast model and a 3D-Var scheme in the assimilation system (Fujiwara *et al*., 2017). The horizontal resolution is T62 Gaussian grid with 192 × 94 grids of the overall data set (∼ 1.875°);
- NCEP-R2 (Kanamitsu *et al*., 2002) was released in 2000, covering the satellite era and using a version of the same model with corrections for some notable errors and limitations identified in NCEP1. Although both reanalyses remain in use; these systems have some limitations such as relatively low top levels (3 hPa) and coarse vertical resolutions (28 levels). This reanalysis is available at a ∼ 1.875° horizontal resolution.

A fair comparison between station points and gridded products is often a challenge, and there is no specific procedure recommended for it (Maraun *et al*., 2010). In this work, all data sets were resampled into the stations network irregular grid (considered as the reference data set) by considering the closest grid cell of each data set in its native spatial resolution similar to the procedure adopted by other studies (e.g., Acharya *et al*., 2019; Krauskopf and Huth, 2020; Sheridan *et al*., 2020). However, a sensibility study on the comparison procedure was initially performed by resampling all data sets into a regular grid with different methods (bilinear interpolation and nearest neighbour). This analysis showed coherent results among approaches and therefore will not be shown in the present work.

Finally, taking into account that SSA is a wide region with different climates, the total domain (TD) was divided into five sub-regions based on the regionalization of temperature and precipitation daily extreme events by Olmo *et al*. (2020). This regionalization covers the three regions selected in SSA by Iturbide *et al*. (2020) for the IPCC updated climate reference regions and presents more restricted sub-regions in order to better describe their different climatic characteristics. The regions considered are northern Chile (32 stations), central and southern Chile (20 stations), the arid diagonal region of Argentina (34 stations), Argentinian Patagonia (28 stations) and southeastern South America (118 stations) (R1 to R5, respectively, presented in Figure 1).

## 2.2 | Methodology

Since the aim of this study is to compare climatic characteristics and changes of the above mentioned surface variables represented in a set of reanalysis, a subset of indices from the expert team on climate change detection and indices (ETCCDI, Klein Tank *et al*., 2009) and two other user-defined indices were evaluated (see Table 2 for their description), covering the average and extreme behaviours of daily precipitation, TN and TX. Precise information on ETCCDI indices can be found on http://etccdi.pacificclimate.org/indices.shtml. All indices were calculated annually for every grid cell and for each meteorological station in SSA. Percentile-based indices were constructed considering the base period 1979–2017. The calculation of indices were implemented by using the R-based climate4R open framework (Iturbide *et al*., 2019).

To determine the presence of monotonic upward or downward trends in the regional average series, the non-parametric Mann-Kendall test was implemented (Mann, 1945; Kendall, 1975). The performance of the

**TABLE 2** Temperature and precipitation indices analysed in this study

| Index | Definition | Units | Reference |
|---|---|---|---|
| **CDD** | Maximum number of consecutive dry days (RR < 1 mm) | Number of days | ETCCDI (Klein Tank *et al*., 2009) |
| **CWD** | Maximum number of consecutive wet days (RR > = 1 mm) | Number of days | |
| **DTR** | Daily temperature range | °C | |
| **PRCPTOT** | Total precipitation in wet days (RR > = 1 mm) | mm | |
| **R10mm** | Count of days when RR > = 10 mm | Number of days | |
| **R95p** | Total precipitation when RR > 95th percentile | mm | |
| **Rx5day** | Maximum consecutive 5-days precipitation | mm | |
| **TN10p** | Percentage of days when TN < 10th percentile | % | |
| **TN90p** | Percentage of days when TN > 90th percentile | % | |
| **TNn** | Minimum value of daily minimum temperature | °C | |
| **TNx** | Maximum value of daily minimum temperature | °C | |
| **TX10p** | Percentage of days when TX < 10th percentile | % | |
| **TX90p** | Percentage of days when TX > 90th percentile | % | |
| **TXn** | Minimum value of daily maximum temperature | °C | |
| **TXx** | Maximum value of daily maximum temperature | °C | |
| **TNm** | Mean value of daily minimum temperature | °C | User-defined |
| **TXm** | Mean value of daily maximum temperature | °C | User-defined |

*Note:* All indices were calculated annually during the period 1979–2017 (39 years).

different data sets in representing the interannual variability was assessed using the Spearman's rank correlation (Spearman, 1904) statistically tested at the 95% level of significance (Wilks, 2011). The correlation was computed using the linearly detrended time series. Note that reanalyses are not long-term homogeneous and therefore special caution must be taken when analysing trends (Sterl, 2004; Thorne and Vose, 2010). However, it is important to keep in mind that the purpose of this work was to evaluate and inter-compare different aspects of reanalyses, including trends, and not to estimate the long-term climatic changes using reanalyses.

Additionally, Taylor diagrams (Taylor, 2001) were used for summarizing the representation of the spatial distribution of the climatological fields of PRCPTOT, TNm and TXm. These diagrams quantify the degree of statistical similarity between the reference observations and the rest of the data sets, by reporting the Spearman correlation coefficient, the ratio of the standard deviations and the centred root-mean-squared-error (RMSE).

## 3 | RESULTS

### 3.1 | Mean fields: PRCPTOT, TXm and TNm

The spatial mean and bias fields of the indices related to mean conditions PRCPTOT (total annual accumulated precipitation), TXm and TNm (annual mean TX and TN, respectively) were initially compared (Figure 2a). Spatial differences of these indices compared with the STN data set were quantified through Taylor diagrams presented in Figure 2b. Results indicated that reanalysis relatively well represented the spatial distribution of the climatological patterns in SSA (mean fields in Figure 2a). The spatial structure of both extreme temperature mean fields, characterized by a southwest-northeast gradient as consequence of the Andes range, was successfully captured by reanalyses. However, some differences could be observed in the biases fields of Figure 2a. All reanalyses presented an intensified SW–NE gradient for TNm, with warm biases in southeastern South America (R5) and in the north of Argentinian Patagonia (R4) and cold biases in the southern portion of SSA (R2 and R4) and in the east of the Andes mountain range. In the case of TXm, negative biases were observed in the southern tip of the continent and near the Andes range (R1 and R3). This was detected in all reanalyses but especially in JRA55, NCEP1 and NCEP2, that presented generally the coldest biases while exhibiting warm biases in the centre of R5. ERA.INTERIM and ERA5 showed minor biases, except for the portions of R1 and R3 near the Andes range. When analysing the differences between the two observational data sets, the largest biases in TXm and TNm mean fields were observed near the Andes range, mainly in the stations close to central Chile at the south of R1 where CPC tended to show lower values than STN, evidencing the observational discrepancies in regions with such complex topography.

In the case of the precipitation fields, although reanalyses were able to place the maximum precipitation areas in southern Chile and in southeastern South America (R2 and R5, respectively) (mean fields in Figure 2a), overestimations were evident mainly for ERA.INTERIM, ERA5 and JRA55 for the former region and near the Andes in northern Chile and Argentina. Wet biases were present in all reanalyses over the southern section of the Andes Mountains, in southern Argentinian Patagonia and in some portions of northern Argentina in the eastern side of the Andes. However, note that in regions R1, R3 and R4 precipitation amounts are low and relative differences may exacerbate the biases. In addition, some overestimations were probably due to difficulties in representing the physical mechanisms involved in the precipitation occurrence (Dulière *et al*., 2011), which was particularly evident for orographic precipitations in SSA. In particular, ERA.INTERIM differed from the rest of the reanalyses in eastern and central Argentina (R3 and south of R5) where this data set showed extended wet biases for PRCPTOT. In the case of NCEP1 and NCEP2, drier biases were observed in R5 and in central Chile. Regarding the comparison between CPC and STN, the largest differences were again observed along the Andes range.

Taylor diagrams of mean fields considering the total domain as a whole (Figure 2b) showed that correlations reached values around 0.9 for TNm and lower values for TXm and PRCPTOT. In the latter, the spread in the cloud of points increased and ERA.INTERIM showed the lowest correlation values and also the highest RMSE. In terms of spatial dispersion, depicted by the standard deviation considered as a global metric across SSA, reanalyses tended to underestimate it for the temperature variables. In addition, all reanalyses generally exhibited a similar behaviour for TXm and TNm, as it can be seen in the different clouds of points. As it was expected, CPC results were better than the ones found for reanalyses as the distance to the observational reference was clearly shorter for the three variables in the Taylor diagrams. It is interesting to note that the agreement between CPC and STN was very good for the three indices analysed, showing closer points to the STN reference than the reanalysis data sets particularly for PRCPTOT.

Note, however, that the evaluation of the Taylor diagrams in Figure 2b over the total domain may mask some

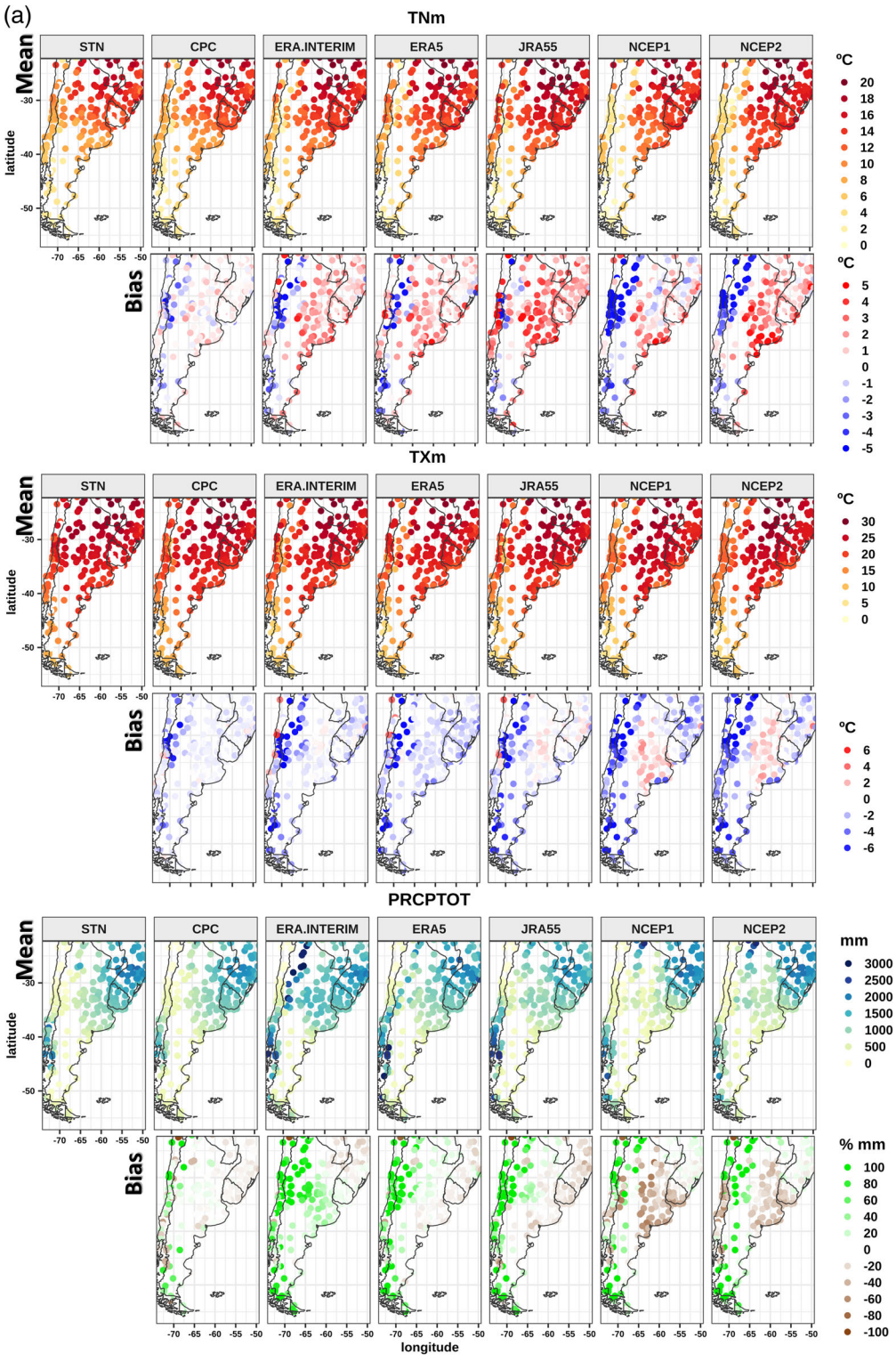


**FIGURE 2** Mean fields and biases compared with STN for TNm, TXm and PRCPTOT during the period 1979–2017: (a) spatial pattern; (b) Taylor diagrams [Colour figure can be viewed at wileyonlinelibrary.com]

misrepresentations by the different reanalysis data sets as evidenced in the biases in Figure 2a. Taking this into account, Taylor diagrams for these indices over each region over SSA were included as supplementary material to complement this analysis (see Figure S1). It is important to mention that in some regions, the number of station points considered to calculate the diagrams metrics is low (and in some cases unevenly distributed)

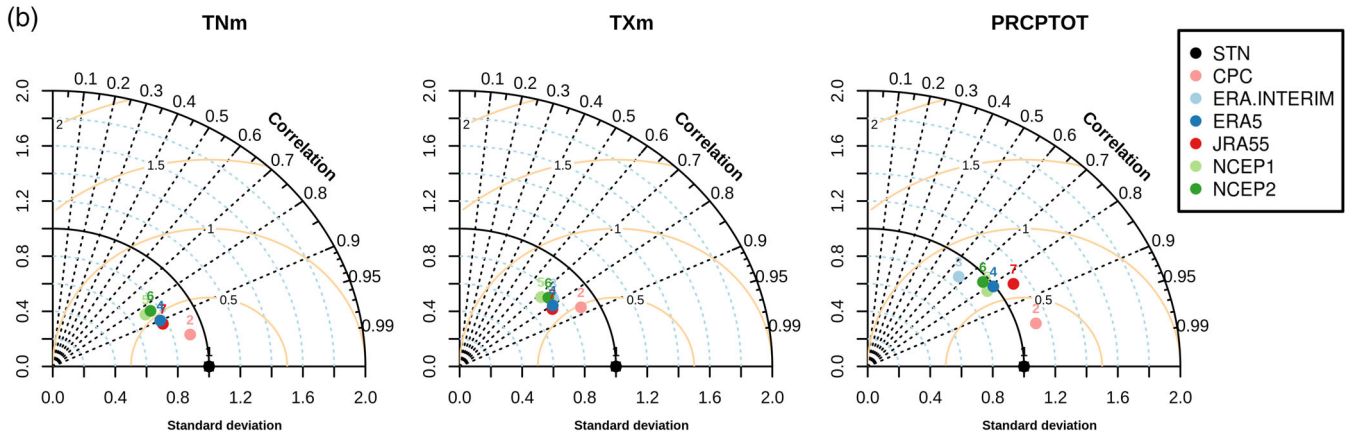


FIGURE 2 (Continued)

and therefore the statistics cannot be considered robust enough to give an exact measure of the reanalyses performance. For instance, R4 consisted in 28 station points notably dispersed over the whole region. Moreover, there were 32 stations over R1, a region with large elevation differences among nearby stations, many of them over the highest areas of the Andes, which are commonly not well represented by the closest grid cell of the reanalyses due to poor spatial resolution. This was reflected in the Taylor diagram of R1 due to low spatial correlations, even negative in the case of TXm. Other discrepancies with the total domain metrics were found particularly over R3 for the three indices—with lower correlations and larger RMSE—and a larger cloud of points for PRCPTOT over R2 and R4. R5 depicted congruent results to the total domain (Figure S1), which was probably related to the larger availability stations points (118).

These results evidenced, to some extent, the lack of reliable high-quality observational data in SSA. Any available observation-based record is only some approximation of the true state of atmospheric quantities due to the different sources of uncertainties (Kotlarski *et al.*, 2019). Therefore, the use of multiple reference data sets would be recommendable to assess reanalysis performance. In this work, additionally to the stations network (which was used as reference), the CPC data set was included for comparison purposes. However, it is worth mentioning that other satellite-based data sets are available for daily precipitation covering the whole SSA domain (Condom *et al.*, 2020), but unfortunately, they are not available for daily temperatures, which limits studies like the one proposed in the present work. In this regard, Taylor diagrams provide objective measures of observational uncertainties given by the distance between CPC and the reference point (in this case STN) in the cloud of points. Furthermore, large uncertainties among all data sets were evident in northern Chile (R1) in the three variables of interest (Figure S1) associated with the complexity of this region in terms of topography. In southern Chile (R2), large uncertainties were evident for PRCPTOT as observed in the Taylor diagram of R2 (Figure S1) and the large biases over the region (Figure 2), probably related to representativity issues of rainfall measurements in a region of such complex topography and high precipitation amounts. In turn, southeastern South America (R5) is the region of SSA with the largest number of available meteorological stations (Figure 1) and also one with the lowest uncertainties in the mean field of PRCPTOT, TNm and TXm (Figure S1). In spite of this, large observational uncertainties were reported in previous studies regarding the definition of the location and intensity of extreme precipitation events that characterized the region (Bettolli *et al.*, 2020), indicating that observational uncertainties were not only related to spatial coverage of meteorological stations but also with the physical nature of the climate phenomena of interest.

## 3.2 | Spatial patterns: Extreme indices

As for the indices described in Section 3.1, the annual mean indices and their biases compared with the STN for the rest of the data sets are presented in Figure 3a for TN extremes. Most of the data sets well captured the latitudinal gradient of annual extremes in minimum temperature observed in STN and CPC. For TNn, values below zero extended from Argentinian Patagonia (R4) up to subtropical latitudes east of the Andes, whereas northern Chile (R1) and southeastern South America (R5) presented temperatures above zero. Meridional transport of air masses in both senses is intense in the eastern side of the Andes due to the mountains completely block the westerly flow in the

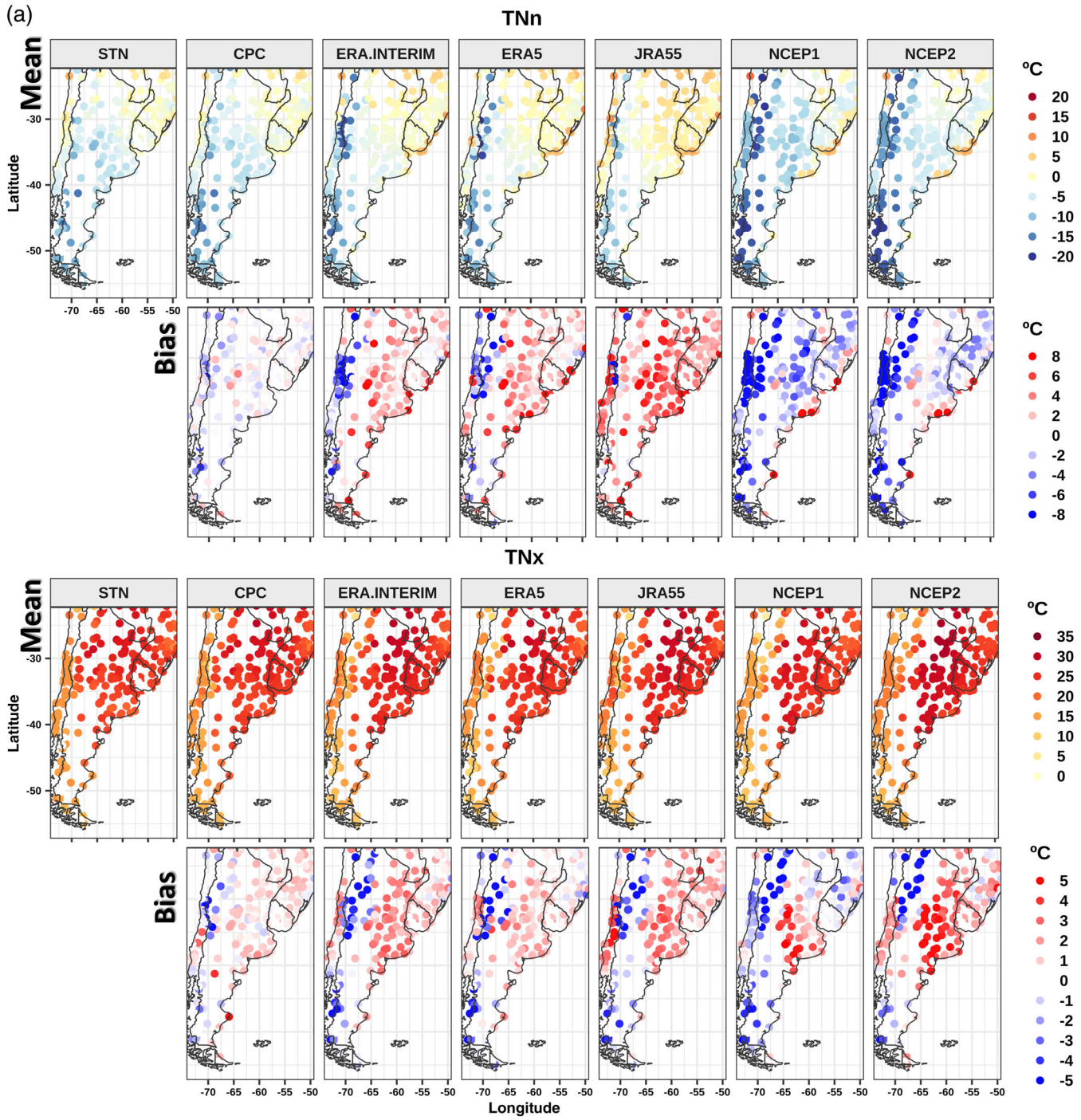


**FIGURE 3** Annual mean temperature indices and biases compared with STN during the period 1979–2017, as obtained from the different reanalyses and observational data sets: (a) minimum and maximum TN; (b) minimum and maximum TX [Colour figure can be viewed at wileyonlinelibrary.com]

lower troposphere and tend to channel the transport of air masses in both senses (Seluchi and Marengo, 2000) allowing cold incursions from high latitudes to penetrate into subtropical and tropical South America (Espinoza *et al.*, 2013). These features may be misrepresented by all reanalysis data sets as per the extreme minimum temperature magnitudes. On one hand, both NCEP1 and NCEP2 generally underestimated this index resulting in a generalized colder pattern, particularly in the arid diagonal region of Argentina (R3), southern Chile (R2) and in Argentinian Patagonia (R4). This was highlighted in the biases, where NCEP1 and NCEP2 presented the lowest temperatures in those regions with underestimations of more than 5°C. NCEP1 exhibited generalized negative biases except for

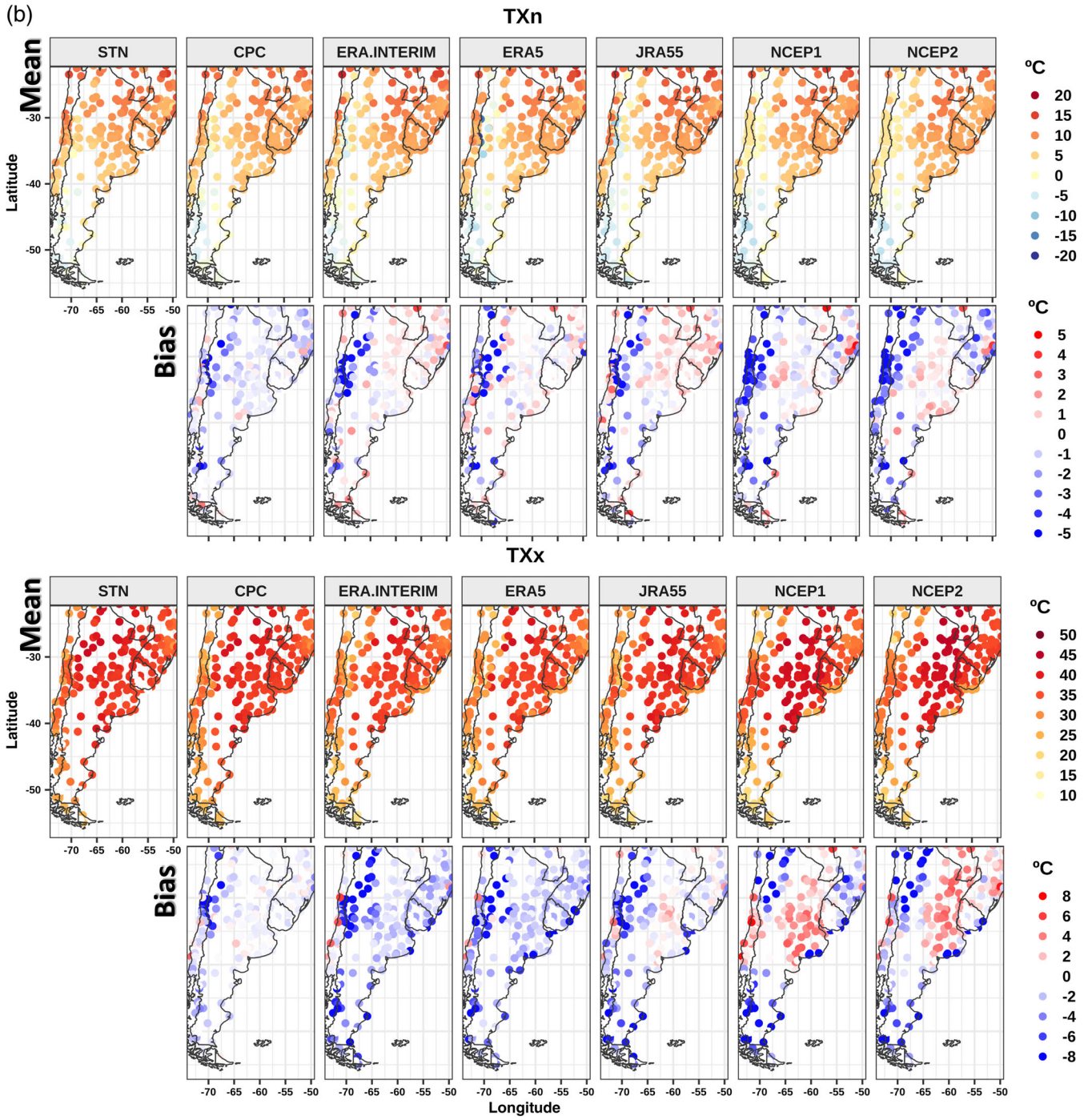


FIGURE 3 (Continued)

the coastline portion of Southeastern South America. On the other hand, ERA.INTERIM, ERA5 and especially JRA55 overestimated TNn over large portions of SSA. Particularly, JRA55 presented positive biases in all regions, except for a few stations in R1. In this index, CPC, presented differences with STN along the Andes mountain range (R2 and R1).

For TNx, higher spatial agreement (in terms of the sign of the biases) among the reanalyses was observed. All reanalyses exhibited positive biases in R5 and in northern Argentinian Patagonia (R4) while cold biases in the southern part of SSA and in the arid diagonal region of Argentina (R3). All of the reanalyses but NCEP1 presented warm biases of about 3°C over central Chile, more pronounced in JRA55. In relation to CPC, this data set presented slight positive differences with STN over most of SSA, but typically smaller than the ones detected in the reanalyses except for few stations over R4. In addition,

colder TNx were found over the Andes mountain range in R3 compared with the stations reference.

Figure 3b exhibits the results for the annual extremes of TX. Although the general structure of the mean fields were captured by all data sets, some systematic biases were observed. In the case of TXn, the index values over the central part of the Andes mountain range and in the arid diagonal region of Argentina (R1 and R3) were underestimated by all reanalyses. The pronounced negative biases in NCEP1 and NCEP2 were more extended over Chile and the arid diagonal region of Argentina (R3) in congruence with the cold biases observed for TNn (Figure 3a). On the other hand, in the north of southeastern South America (northern R5), the reanalyses ERA.INTERIM, ERA5 and JRA55 slightly overestimated the value of TXn, being more noticeable in JRA55. For this index, CPC showed generally negative differences with respect to STN, intensified over the highest elevation areas of R3.

In the case of TXx (Figure 3b), the different data sets showed a general agreement in the mean field, however the spatial pattern of the biases pointed out the differences among reanalyses. In most of R5, NCEP1, NCEP2 and—to a lesser extent—JRA55 presented warm biases (greater than 4°C in some areas), whereas ERA.INTERIM and ERA5 tended to slightly underestimate TXx in this region. Generally, cold biases were found in Argentinian Patagonia (R4), intensifying the meridional temperature gradient observed in the mean field, especially in NCEP1 and NCEP2. Over central Chile, NCEP1 overestimated TXx, while both ERA reanalyses and JRA55 tended to underestimate this index. In addition, CPC, exhibited a higher underestimation of TXx in this portion of the Andes, evidencing the complexity of the region.

Indices associated with precipitation are displayed in Figure 4. For R10mm, STN indicated that in about 60–80 days in a year, precipitation is higher than 10 mm in both rainiest regions in SSA (R2 and R5) (Figure 4a). ERA.INTERIM, ERA5 and JRA55 overestimated the index in R2, while the first one also exhibited pronounced wet biases in the arid diagonal region near the Andes, with overestimations in the frequency of heavy rainy days of more than 30 days. The same was found for NCEP1 and NCEP2 that, in addition, presented wet (dry) biases in the northeastern (southwestern) portion of R5. In the case of R95p, which is associated with extreme events in terms of the accumulated precipitation, large differences were found alongside the Andes for ERA. INTERIM, ERA5 and JRA55, that exposed greater accumulated precipitation than the observations. Note that, for both precipitation indices, CPC exhibited the closest values to STN, although some differences were evident near the Andes. NCEP1 failed to interpret the spatial behaviour of R95p and generally underestimated it, whereas NCEP2 tended to overcome this shortcoming with lower underestimations in R5 but presented notable wet biases along the mountains over R3 and also over Argentinian Patagonia (R4). The latter was systematically found in all data sets. ERA.INTERIM greatly overestimated the values of the precipitation indices over the western area of R3 along the Andes mountain range, however, this misrepresentation seemed to be improved in the new generation of the European reanalyses, in which wet biases were reduced and confined only to the nearest area to the Andes.

Overestimations in R10 and R95p over southern Chile (R2) were in agreement with the overestimations observed in PRCPTOT over this region, particularly by ERA reanalyses and JRA55 (Figure 2), indicating that large precipitation amounts in these reanalyses were due to more frequent heavy and extreme precipitation over the region. Southern Chile is one of the rainiest regions in South America after the Colombian Andes and the Amazonian region. It is influenced by westerly winds throughout the year in such a way that moisture in Pacific air masses falls upwind of the topographic barrier, with accumulated annual values over 2000 mm (see PRCPTOT in Figure 2). In this regard, although a process-based analysis is beyond the scope of this work, these results suggest that ERA reanalyses and JRA55 may have difficulties in reproducing the physical mechanisms that lead to precipitation over this region. In the same way, over southeastern South America (R5) diverse forcings in different temporal and spatial scales influence precipitation occurrence and intensity, associated with extratropical synoptic activity, cyclogenesis and mesoscale convective systems features that are dominant in the different seasons of the year (Cavalcanti, 2012). The complexity of the climatic features that lead to precipitation over this region poses a challenge to dynamic modelling, and in particular to reanalyses as shown here.

In the case of dry and wet spells (CDD and CWD, respectively, in Figure 4b), all data sets indicated the largest CDD in northern Chile and in the arid diagonal region, in coherence with the characteristics of those arid regions. However, NCEP1 presented higher CDD values over R3, northern R4 and most of R5. Similarly, NCEP2 exhibited a less pronounced overestimation of the index in southern South America (R5). Commonly, the rest of the reanalyses tended to underestimate CDD over most of SSA but more intensified in the highest elevation areas. For CWD, all reanalyses presented a larger number of days in R2 and also in R3 in the case of the ERA reanalyses, in agreement with the overestimation found in the previously described precipitation indices. Moreover, NCEP1 and NCEP2 showed the largest differences in R5 with spells up to 80 days, which was not seen neither in STN nor in CPC. The largest differences between

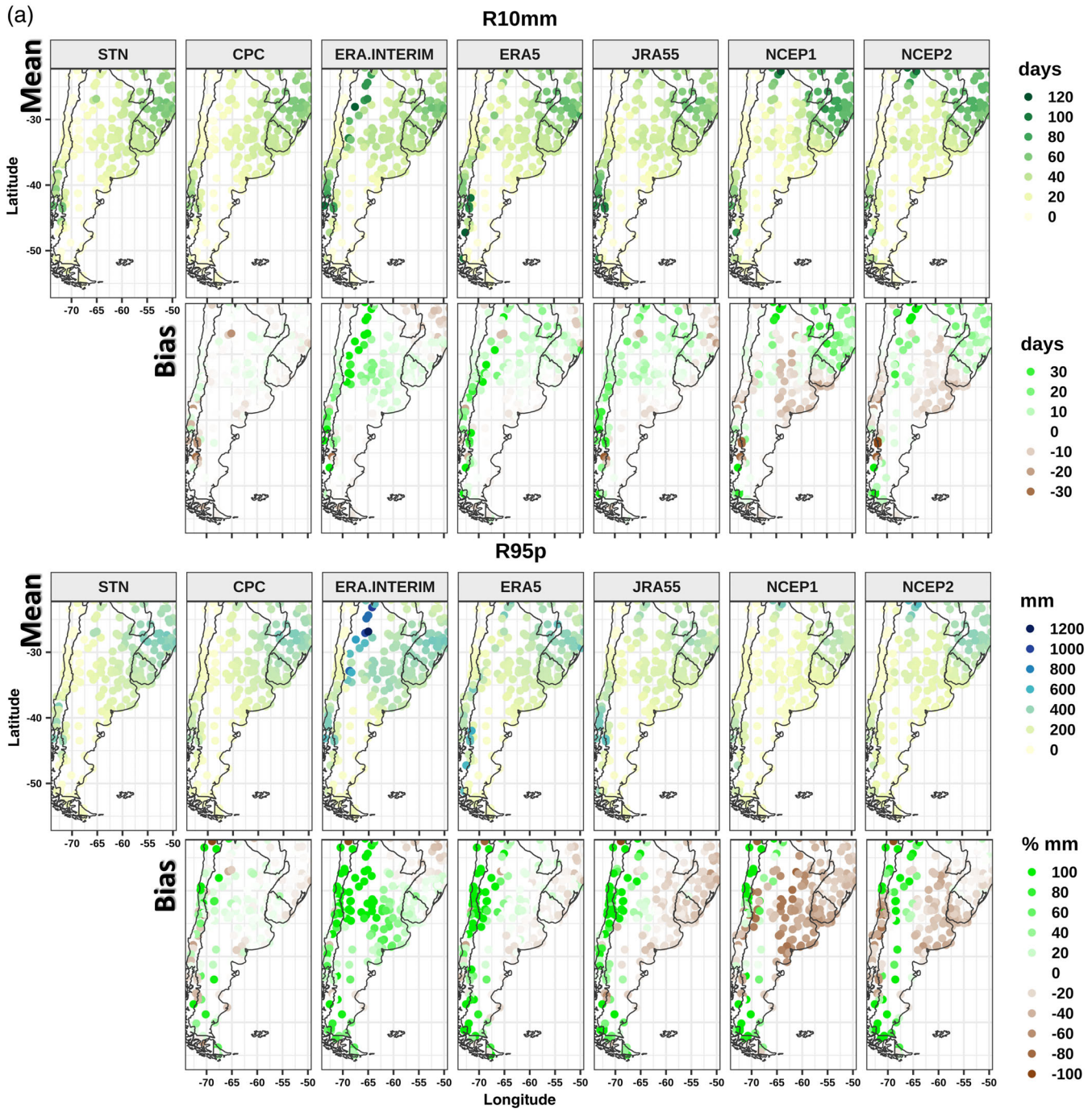


FIGURE 4 Annual mean precipitation indices and biases compared with STN during the period 1979–2017 as obtained from the different reanalysis and observational data sets: (a) R10mm and R95p; (b) CWD and CDD [Colour figure can be viewed at wileyonlinelibrary.com]

CPC and STN were found for the CDD index, especially over central Chile.

## 3.3 | Trends

Kendall-Tau values as representative of trends of the regional average series of all the indices indicated in Table 2 are shown in Figure 5. Trends are presented by data set, in the total domain (TD) of SSA and in each region for the closest grid cell to each station (Figure 5).

Taking into account the total domain (TD) (Figure 5), TXx and Tx90p were the only indices in which most of the reanalyses agreed in positive and significant trends, in accordance to STN and CPC. Similarly, TXm presented positive trends in the majority of the data sets, but for this

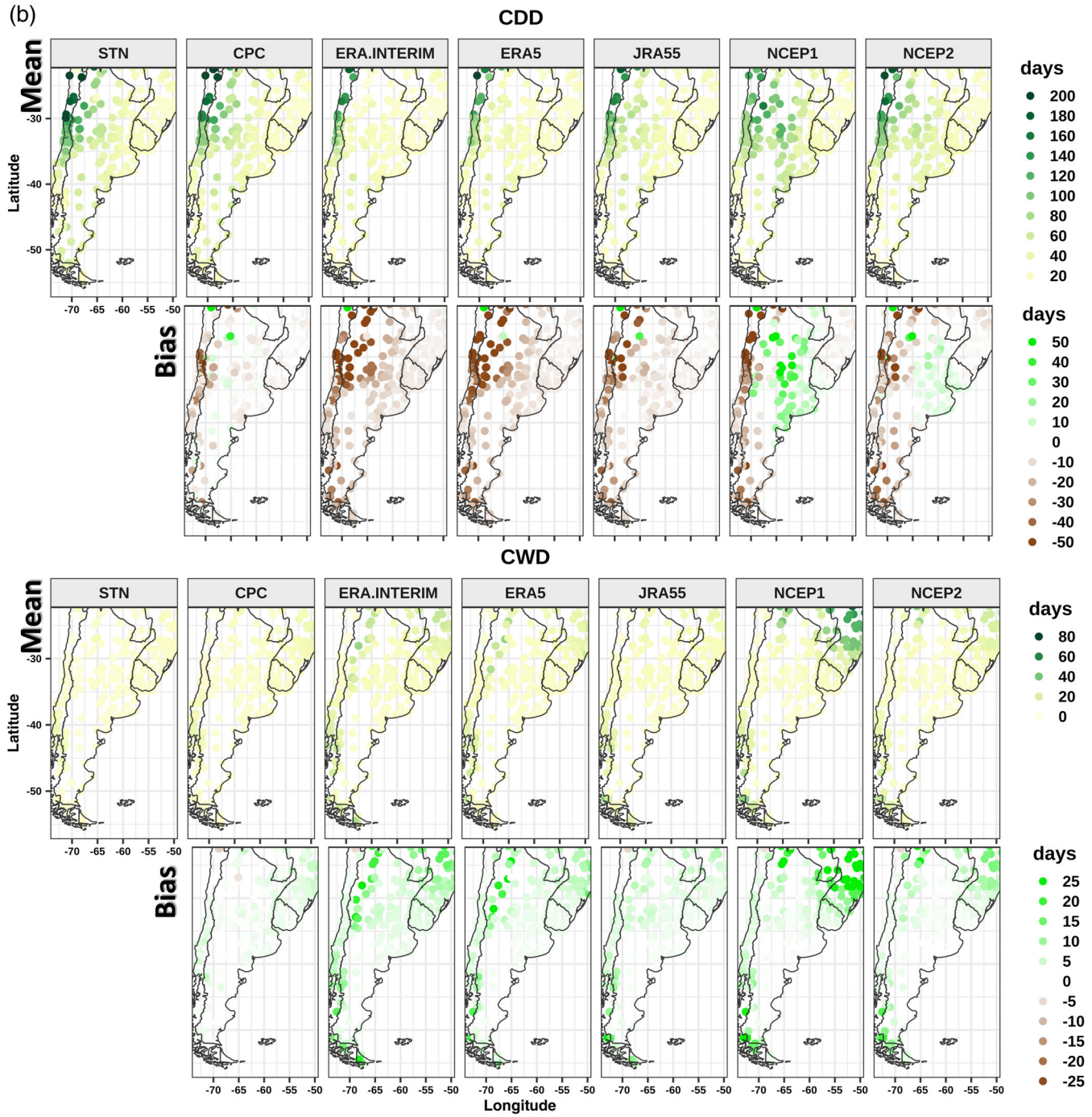


FIGURE 4 (Continued)

case not significant in JRA55. However, for these indices, NCEP1 and NCEP2 presented contrary trends to the rest of the data sets. These discrepancies were observed in almost all the indices related to maximum and minimum temperatures. For the particular case of TXx, Donat *et al.* (2014) found trends of contradictory signs for NCEP1 in South America when compared with different data sets. The authors pointed out that this could be associated with erroneous maximum temperatures in this data set between the 1980s and the mid-1990s, which had been already recorded in other regions by other authors (Kharin *et al.*, 2005; Sillmann *et al.*, 2013). Furthermore, Dufek *et al.* (2008) found a similar behaviour in NCEP1 for the frequency of cold nights (TN10p) in most parts of Argentina during 1961–1990, and attributed this difference to model inefficiencies such as surface processes representation, resolution and others. However, in the present study a similar performance to NCEP1 was also

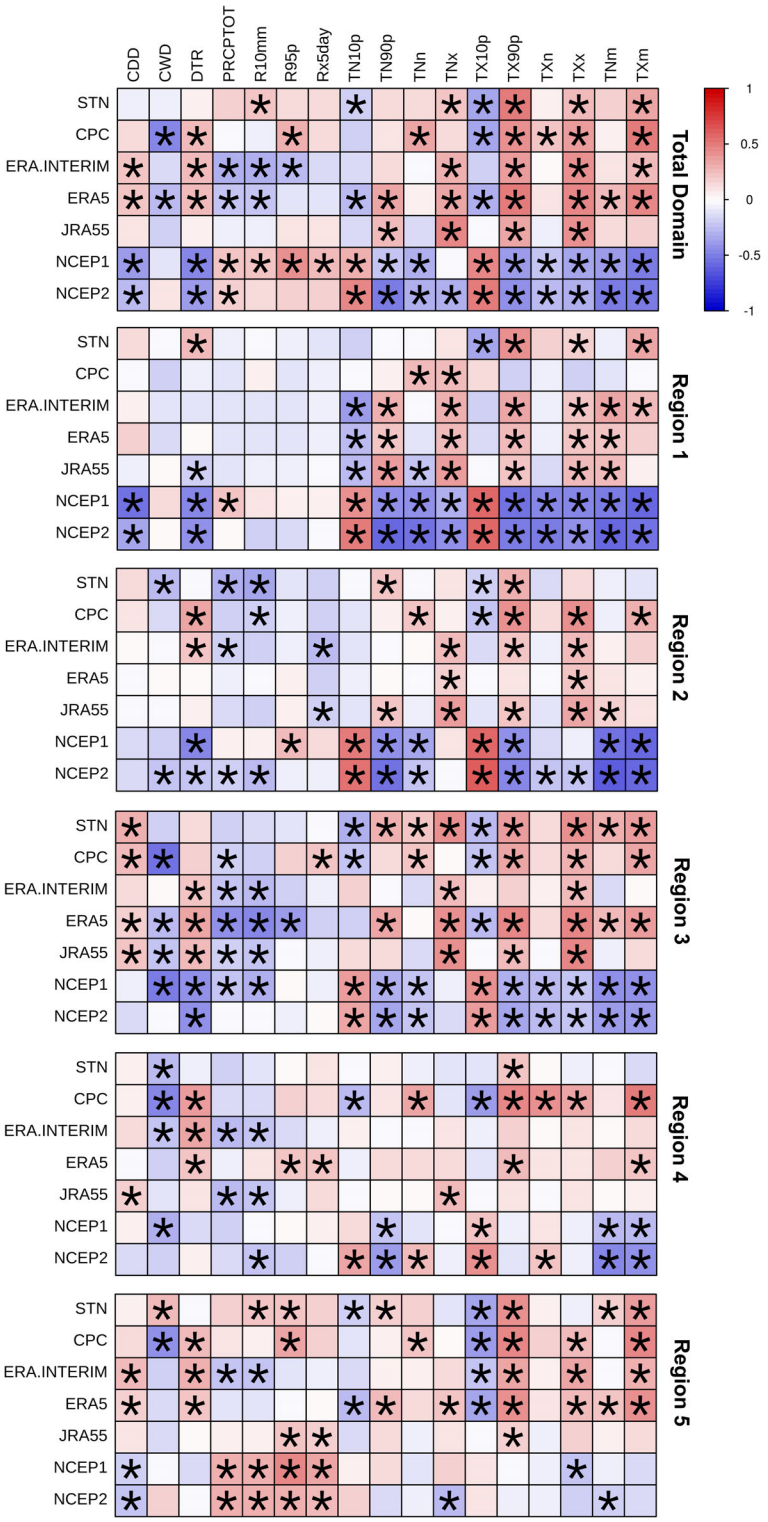


**FIGURE 5** Kendall-Tau values as representative of trends on the regional average annual series of the indices during the period 1979–2017. Significant trends at the 90% level of significance are marked with an asterisk [Colour figure can be viewed at wileyonlinelibrary.com]

observed for NCEP2 when considering the different indices associated with maximum temperature and minimum temperature as well. These results will be discussed in more detail in Section 3.4.

The minimum temperature index TNx also exhibited significant upward trends in the total domain for STN, ERA5, JRA55 and ERA.INTERIM, whereas TN90p only presented significant results in ERA5 and JRA55 (Figure 5). When evaluating cold extremes, TN10p and TX10p showed significant downward trends in STN and in CPC for the case of TX10p. Regarding the reanalyses, these trends were only well represented by ERA5. Trends of TNn and TXn were weaker and only significant in CPC. DTR showed significant positive trends

in CPC, ERA.INTERIM and ERA5 but it was not significant in the case of STN. NCEP1 and NCEP2, in contrast, presented a negative and significant trend for this index.

In spite of NCEP1 and NCEP2 results for extreme temperature indices, warming conditions were generally found over SSA considered as a whole subcontinental region, which may be explained by both changes in the intensity and frequency of extreme temperature events. These results were in line with the ones found by other authors, mostly for TN90p and TN10p (Vincent *et al*., 2005; Skansi *et al*., 2013; Donat *et al*., 2016; Olmo *et al*., 2020). However, some contrary results were obtained in the case of the indices related to TX. Donat *et al*. (2016) analysed TXx and TX90p over the past century and found no signal of warming in southern and western South America. Furthermore, Skansi *et al*. (2013) identified weak trends in SSA, negative for TXx in the period 1960–2010, and positive for TX90p, especially in Argentina. More generally over South America, the authors distinguished a faster rate of warming in the TN-based indices than in the TX-based indices. It is worth noticing that this was not observed in the present study. On the contrary, the indices associated with TX presented predominantly higher and more homogeneous trends than the TN-based indices (Figure 5). Olmo *et al*. (2020) already addressed these discrepancies in SSA and mentioned that they could be related mainly to the sensitivity of trends to the period of study, and also to the one used to construct the percentile-based indices. Notwithstanding, in the present study a sensitivity study was performed changing the base period from 1979–2017 to 1981–2010, and differences within the series of the percentile-based indices were negligible. This indicated that our results were consistent considering a different base period than the total period of study.

Trends in precipitation indices in SSA were less consistent than for temperature indices (Figure 5). The precipitation indices PRCPTOT, R10mm, R95p and Rx5day exhibited positive and significant trends in NCEP1 and for the case of PRCPTOT in NCEP2 too. In particular, STN (CPC) agreed with these trends only for R10mm (R95p). On the contrary, ERA.INTERIM and ERA5 showed significant negative trends for PRCPTOT and R10mm. In the case of CDD, both ERA reanalyses presented upward significant trends, while in NCEP1 and NCEP2 negative and significant trends were observed. In addition, CWD had no significant trend in STN, but presented negative significant trends in CPC and ERA5.

The analysis considering the different regions showed that trends presented a notable spatial variability, except for NCEP1 and NCEP2 that showed a systematic contradictory behaviour, similar than in the total domain. The arid diagonal region of Argentina and southeastern South America (R3 and R5) presented similar results to TD, particularly in the indices related to maximum and minimum temperatures (Figure 5). These regions are the most extended over SSA and seemed to show similar signals in the temperature indices trends. In these regions, the majority of the data sets (including STN) agreed on positive and significant trends for TXm and TX90p and significant downward trends for TN10p and TX10p. Also, R3 and R5 exhibited significant upward trends for TNm and TN90p. Furthermore, all regions presented positive and significant trends for TX90p in STN and in most of the data sets. These results were in agreement with previous studies during the recent period: Rusticucci *et al*. (2016) identified significant increases (decreases) in the frequency of warm (cold) daily extremes over the central portion of Argentina (portions of R3 and R5), whereas Olmo *et al*. (2020) also found these warming signals over other parts of SSA, such as southern Chile and Argentinian Patagonia (R2 and R4).

For precipitation indices, R5 was the only region where CWD, R10mm and R95p had a positive and significant trend in STN, also significant in the case of CPC for R95p, while the rest of the precipitation indices showed slight positive changes which were not significant. Surprisingly, CPC presented an opposite significant change in CWD than the stations reference. Whereas the total annual precipitation did not present marked trends in the recent period, there seemed to be an increase in the frequency and intensity of extreme events. In particular, the wetter signals found in this study as depicted by the number of rainy days (both CWD and R10mm) and also by the total precipitation due to extreme rainfall (R95p) were in agreement with previous studies that, working with different data sets and thresholds, also found predominantly upward trends in extreme precipitation events in southeastern South America during the austral warm season (Re and Barros, 2009; Penalba and Robledo, 2010; Olmo *et al*., 2020). However, our results in the annual series may not reflect the temporal changes found by other authors predominantly during the warm season, probably due to the annual estimation of the indices. These results exhibited the uncertainty in precipitation trends over southeastern South America, in agreement with results by Du *et al*. (2019). This uncertainty may be associated with the different indices, base periods and seasons considered when evaluating the trends. On the other hand, in R3, the reanalyses ERA. INTERIM, ERA5 and JRA55 agreed with CPC and STN in the negative trend of PRCPTOT, though no significance was found for STN. For CDD, a positive and significant trend was found in R3 in the majority of the data sets in agreement with the results found by Skansi *et al*. (2013).

The north region of Chile (R1) according to STN presented a positive significant trend in TXm and TXx while a negative and significant trend in TX10p. ERA5, ERA.INTERIM and JRA55 agreed on these results for TXx. Moreover, both ERA reanalyses and JRA55 coincided with CPC in significant and positive trends for TNx, but not with STN, which presented insignificant changes for this index. In particular, CPC did not agree with the trends observed in the STN in this region, showing significant trends only for TNn and TNx. STN also presented a positive and significant trend for DTR in this region. These results differ from the ones of Vincent *et al.* (2005), who found a decrease in the diurnal temperature range in several stations of northern Chile considering a former period of study (1960–2000).

For southern Chile (R2), STN presented significant upward trends for TN90p and TX90p, both well represented by JRA55 and, in the case of ERA.INTERIM, only for the latter index. Schumacher *et al.* (2020), also found an increase of warm days mainly during the winter season in central Chile (R2) in the period 1980–2015. Even more, the precipitation indices CWD, PRCPTOT and R10mm had significant downward trends, whereas CPC also showed the trend for R10mm and ERA.INTERIM for PRCPTOT. These general downward trends in precipitation over large portions of Chile were congruent with results by other authors in terms of precipitation intensity and frequency (Quintana and Aceituno, 2012; Skansi *et al.*, 2013; Olmo *et al.*, 2020; Schumacher *et al.*, 2020).

In Argentinian Patagonia, warm extremes exhibited similar outcomes to R3 and R5 in STN and in some of the data sets, like CPC, ERA5 and JRA55 for TXx (Figure 5). This increase was in accordance with Rusticucci and Barrucand (2004), who found similar results during the second half of the 20th century in Argentinian Patagonia. As observed in the arid diagonal region of Argentina (R3), STN and most of the reanalyses were in agreement in significant downward trends for CWD, and both ERA reanalyses and CPC in upward trends for CDD.

## 3.4 | Series

In order to analyse the interannual variability as depicted by the different data sets, correlation coefficients between the linearly detrended regional averaged series of all the indices and the STN reference are displayed in Figure 6. In the total domain, most of the correlation coefficients for temperature indices were lower for NCEP1 and NCEP2, except for those associated with the absolute minimum values (TNn and TXn) (Figure 6). The highest correlations were observed in ERA5 and ERA.INTERIM in almost all temperature indices, whereas CPC, JRA55 and both NCEP presented much lower correlations, particularly for TNx, TXx and TX90p. NCEP1 exhibited no significant correlation for TXx and TXm. In the case of precipitation indices, the interannual correspondence between the different data sets and STN seemed to be well represented, except for CWD. Regarding the reanalyses, higher correlations values were observed in ERA.INTERIM and ERA5 and particularly lower in NCEP1 for the precipitation indices. Regionally, the lowest correlation coefficients were observed in Argentinian Patagonia (R4) and southern Chile (R2) in almost all indices, and in northern Chile (R1) in temperature indices. In particular, CWD systematically showed low correlations in all regions, except for R1. CDD also presented very low correlation values in R2 and R4 in almost all data sets, while, in the case of temperature indices, in R1 and R4, almost all data sets (including CPC) showed low agreement for DTR. Again, NCEP1 and NCEP2 presented the poorest performance in representing the interannual variations in almost all regions and indices.

In order to visualize the temporal series, the original regional averaged series for few selected indices are presented in Figure 7. Although a good interannual agreement was observed for TXm and TXx (Figure 7a), all reanalyses and CPC tended to underestimate the indices, more noticeable in the TX mean annual values (TXm). This was remarkable in southern Chile (R2), where all reanalyses distinguished from STN and CPC showing higher underestimations. It was worth noticing the temporal behaviour of NCEP1 and NCEP2 indices, which presented a jump towards colder temperatures around 1998. Although this inhomogeneity in the time series was noticed in all regions and in both indices, it was more evident in R1 and R3 (northern Chile and the arid diagonal region of Argentina). These abrupt decreases were detected in Figure 5 as negative significant trends for these indices based on NCEP reanalyses. On the other hand, the significant upward trend detected in Figure 5 for TXx and TXm with general agreement among data sets over the total domain and in regions R3 and, R5 for the case of TXm, was visually evident in the temporal series.

The time series of extreme temperature frequency indices (TX10p and TX90p) displayed in Figure 7b showed generally less dispersion among the different data sets since by construction they are percentile-based. The exceptions were NCEP1 and NCEP2, which stood out from the rest of the reanalyses due to lower values detected in the beginning of the period and higher values in the end for TX10p, while the opposite was observed for TX90p. As previously discussed, this misrepresentation by the NCEP reanalyses was probably the reason for the significant trends of opposite signs shown

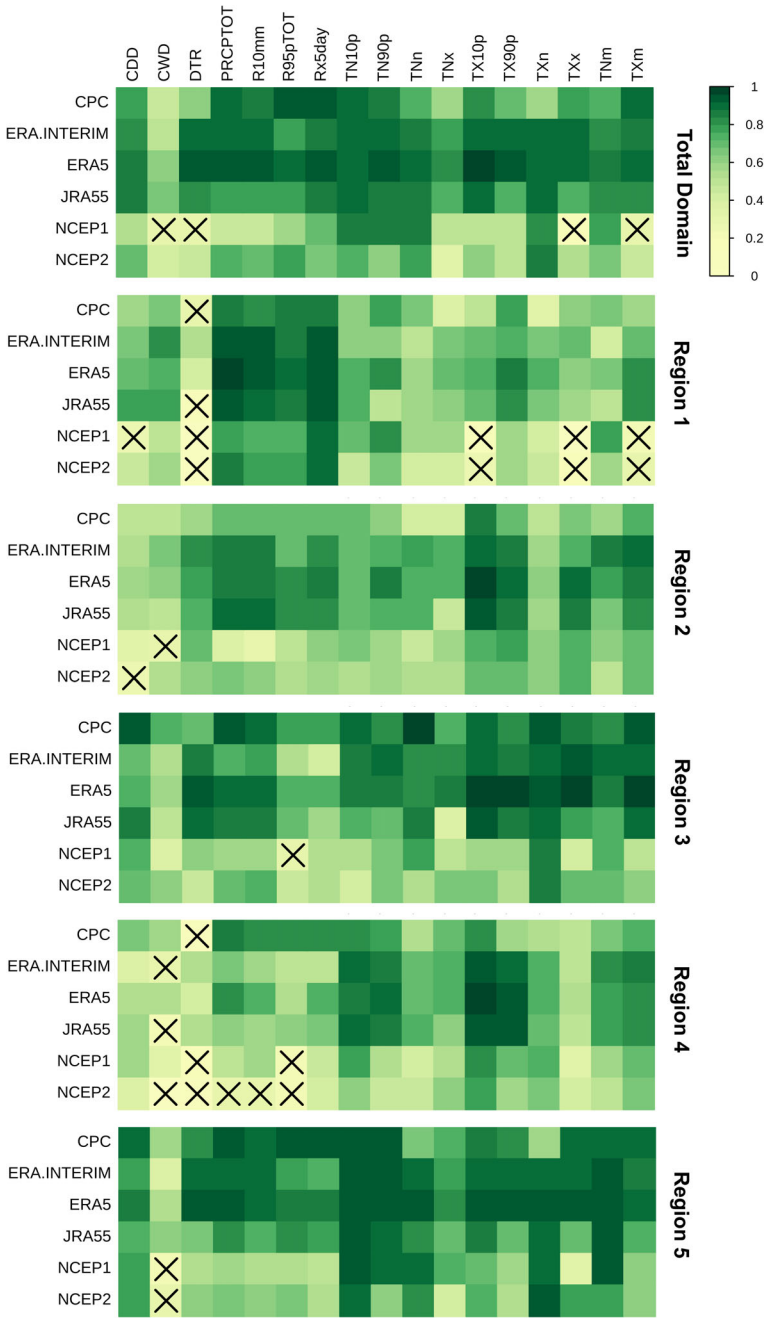


**FIGURE 6** Correlation coefficients between the different regional average annual series of the STN reference and the rest of the data sets during the period 1979–2017. Non-significant values are marked with a cross (95% level of significance) [Colour figure can be viewed at wileyonlinelibrary.com]

in Section 3.3 in most of the regions, more remarkable in TD and in northern Chile (Figure 5). As in TXx and TXm, downward (upward) trends in cold (warm) days in regions R3 and R5 were noticeable from this figure.

In the case of TN indices (see Figure S2a and S2b), a larger spread among data sets was detected, and more disparate results were found among regions, particularly in TNx, which was also reflected in the low interannual correlation values (Figure 6). As it was noted in the TX indices, the jump exhibited in NCEP reanalyses was also observed in TN indices.

In the case of the precipitation indices shown in Figure 7c, the reanalyses performance in reproducing the temporal variability thoroughly depended on the region under consideration. Most of the data sets overestimated R10mm and R95p throughout the Chilean territory (R1 and R2), which was more evident in JRA55 and in the new generation of ERA reanalyses (ERA5). Moreover, in R3, ERA.INTERIM showed the highest overestimations, especially in R95p, evidencing once more the difficulties of this data set in representing the orographic precipitation associated with the Andes mountains. A smaller spread and greater agreement among data sets were observed in R4 and R5 (Figure 7c), particularly in the end of the period of study, which may be related to an increase in the quality and/or quantity of assimilated

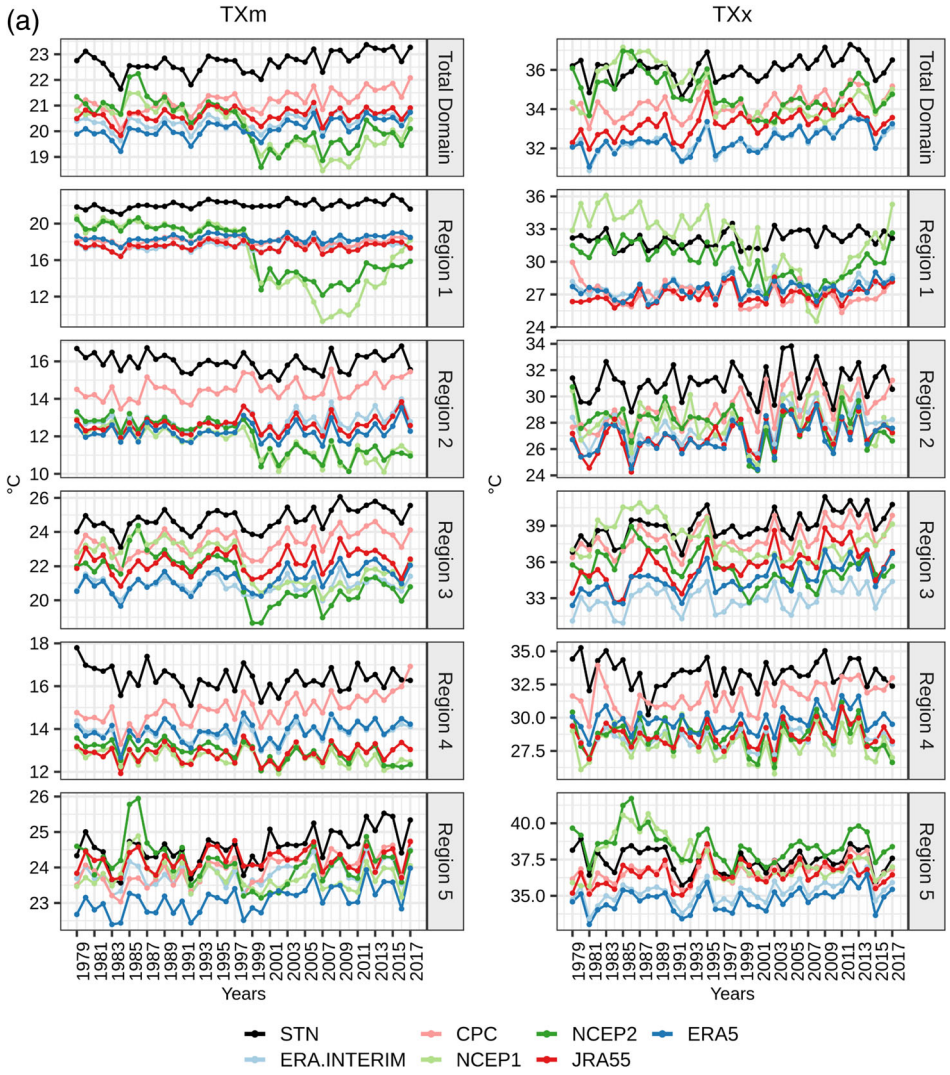


**FIGURE 7** Regional averaged annual series of the indices during the period 1979–2017: (a) TXm and TXx; (b) TX10p and TX90p; (c) R10mm and R95p [Colour figure can be viewed at wileyonlinelibrary.com]

observed data. In R5, it was worth noticing the increase in R10mm and R95p values during the last years of the period (Figure 7c), which was consistent in all data sets, although no significant trends were observed for these indices in the case of the interpolated data (Figure 5). For the dry and wet days spells indices (CDD and CWD, respectively), reanalyses generally underestimated (overestimated) the duration of CDD (CWD) in almost all regions, except for NCEP1, which seemed to overestimate both indices in some regions (see Figure S2c).

## 4 | DISCUSSION AND CONCLUSIONS

Reanalyses represent the observed evolution of weather conditions and provide large spatial and temporal coverage of meteorological data, which make them a well-accepted and useful tool for climate studies. Even more, they are often used in model evaluation due to their gridded output and similarity of scales represented (Sillmann *et al*., 2013). Notwithstanding, they are affected by inhomogeneities in the spatial patterns and temporal evolutions, which may be related to the different processes involved in data assimilation as well as to model uncertainty (Parker, 2016). Hence, intercomparison and evaluation studies against observational data become necessary, particularly in regions like southern South America, where data availability is often sparse (Condom *et al*., 2020). A comparison across multiple data sets may help to bring consistency and ascertain our confidence in changes in extremes (Donat *et al*., 2016).

In this study, several temperature and precipitation indices, with special focus on extremes, were analysed during 1979–2017 using multiple reanalyses, the CPC gridded data set and the most extended network of

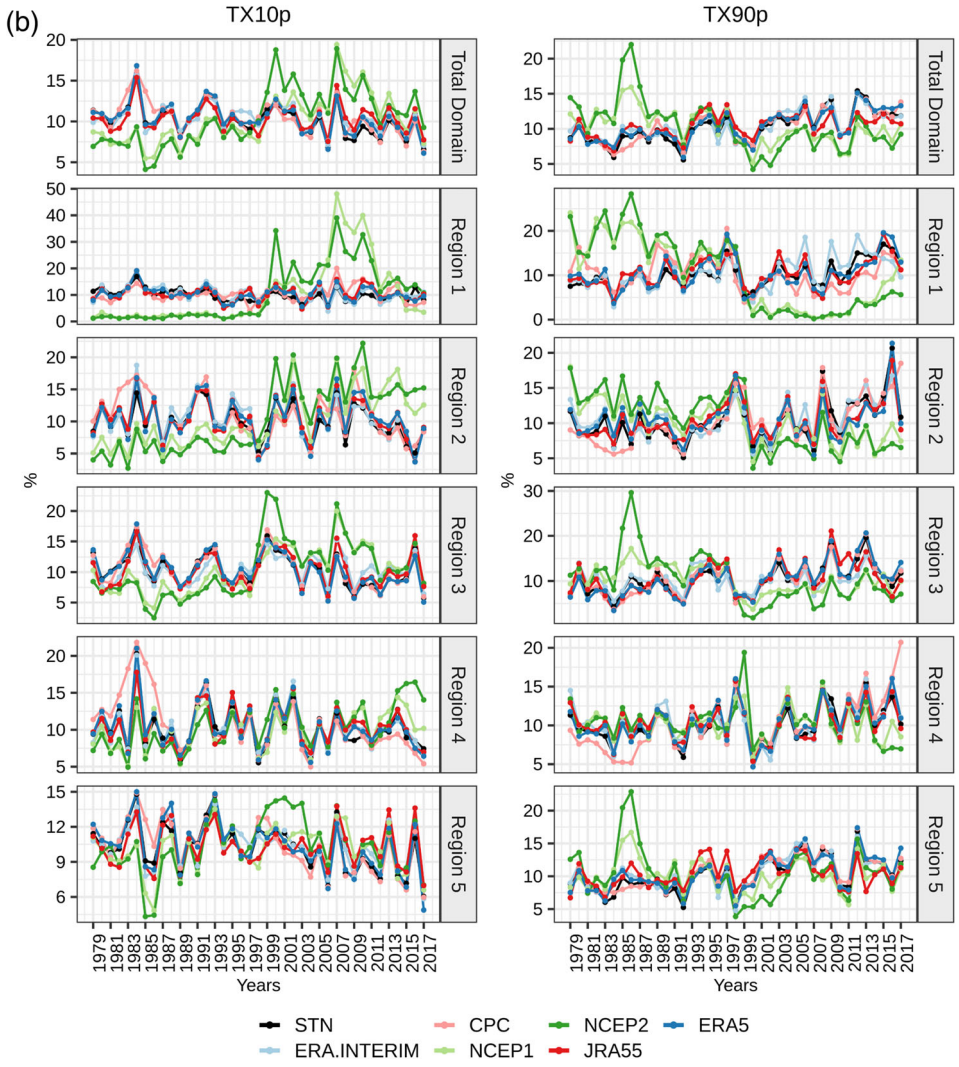


FIGURE 7 (Continued)

meteorological stations used in regional climate studies over southern South America up to date. This was done by addressing the study of their spatial and temporal variability, in particular, the representation of spatial patterns, long-term changes and inter-annual variability. This paper focuses on the different behaviours of the reanalyses rather in the physical and model-construction processes that could be related to them. However, identifying their shortcomings in representing surface variables as well as regions and variables with large uncertainties is a contribution for the understanding of models inefficiencies.

Reanalyses used in this study generally well represented the spatial patterns of most of the temperature and precipitation indices (Figures 2 and 3). However, they tended to overestimate precipitation maximums particularly in southern Chile. ERA.INTERIM strongly overestimated all precipitation indices near to the Andes mountain range. This may be due to an overestimation of wet days frequency and intensity, probably associated with a misrepresentation of the physical processes that lead to orographic precipitation in the region. In the case of temperature indices, NCEP1 and NCEP2 exhibited cooler minimum temperature annual extremes in large portions of southern South America, whereas ERA. INTERIM, ERA5 and JRA55 presented warmer temperatures over the region. Near the Andes mountain range, all reanalysis systematically underestimated the temperature indices. This was also observed for CPC but only in the portion of the Andes close to central Chile, highlighting the large observational uncertainty in this region.

In terms of long-term changes, trends of the regional average series of the indices were analysed (Figure 5). On one hand, most of the data sets considered in this study agreed in general warming conditions over southern South America, more intense in the arid diagonal region

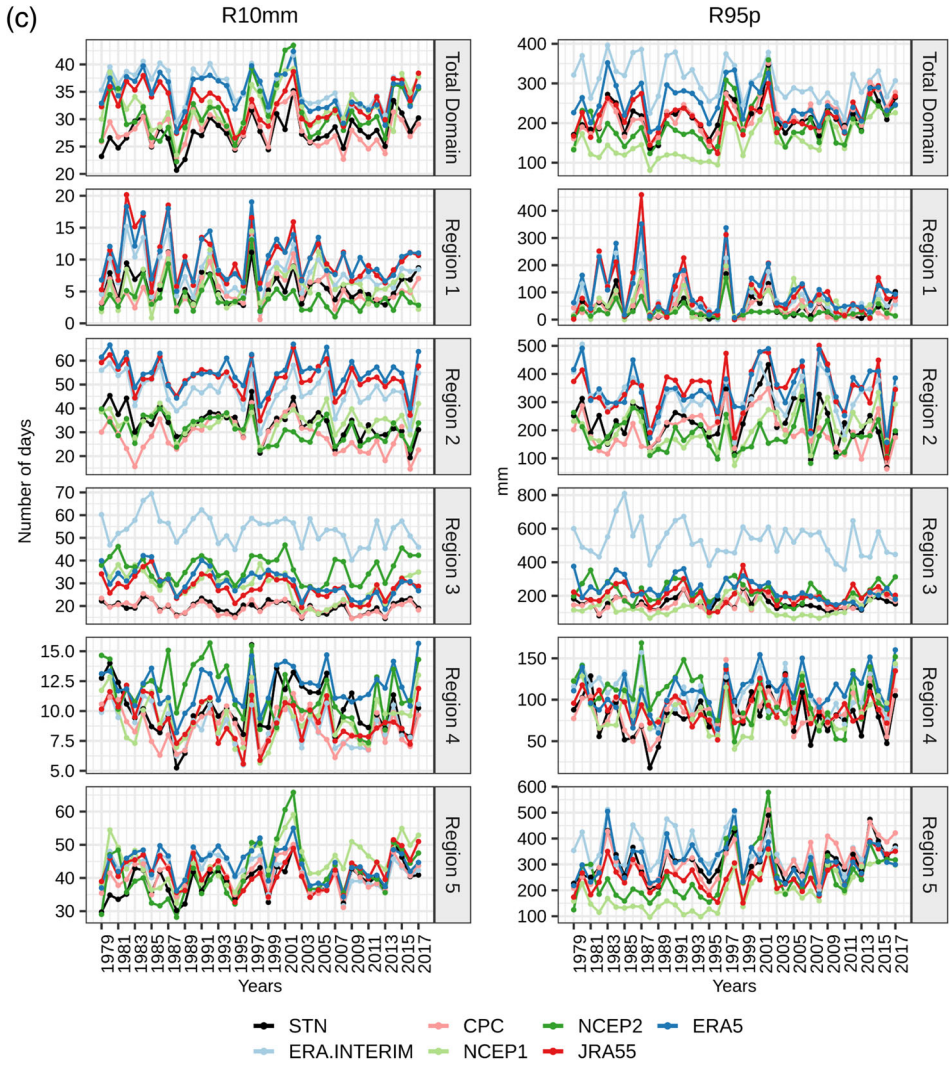


FIGURE 7 (Continued)

of Argentina and in southeastern South America, in accordance with previous studies (Vincent *et al*., 2005; Skansi *et al*., 2013; Donat *et al*., 2016). However, this warming was found to be stronger and more homogeneous in the different regions for the maximum temperature rather than for the minimum temperature, which differed from results by Skansi *et al*. (2013) and Donat *et al*. (2014). These discrepancies were also detected in Olmo *et al*. (2020) during 1979–2015, and may be mainly due to the different and more recent period considered for the estimation of trends. On the other hand, NCEP1 and NCEP2 reanalyses presented contrary temporal changes in almost all the temperature indices. Similar results over different portions of South America were found in NCEP1 for maximum and minimum temperatures extremes by Donat *et al*. (2014) and Dufek *et al*. (2008), respectively, which were probably associated with model inefficiencies, poor representations of surface processes and to resolution. In the present study, we also found this misrepresentation of both extreme temperatures by NCEP2.

In relation to precipitation temporal changes, trends were less significant and consistent than for temperature indices. Wetting signals were identified in southeastern South America as depicted by significant positive trends in the number of days with accumulated precipitation above 10 mm and in the total precipitation above the 95th percentile in STN and also in CPC for the latter index, but results for the rest of the precipitation indices and the reanalyses were unclear. Precipitation trends over southern South America still present uncertainty (Du *et al*., 2019), although significant positive changes were found in previous studies considering different periods and thresholds, particularly in extreme events during the austral warm season (Re and Barros, 2009; Penalba and Robledo, 2010; Olmo *et al*., 2020). In this

work the indices were built on an annual basis, therefore, they may not reflect these temporal changes detected by other authors. In the arid diagonal region, most of the data sets agreed in drier conditions as reflected by significant positive trends for dry spells and negative trends for the total annual precipitation. For southern Chile, general downward trends were found in the total annual precipitation and wet spells for STN and also in the number of days with accumulated precipitation above 10 mm in STN and CPC, although no clear changes were observed in the reanalyses in those indices. These negative trends in precipitation over large portions of Chile agreed with results by other authors (Quintana and Aceituno, 2012; Skansi *et al*., 2013; Olmo *et al*., 2020).

In this context, it was interesting to highlight that trends in extreme indices were highly variable over the different portions of southern South America and often between data sets (Figure 5). Therefore, they should be evaluated regionally for a better understanding of their temporal changes. In this sense, CPC successfully reproduced the observed long-term changes in spite of the changing amount of stations over time used to construct this data set (Xie *et al*., 2007). These results were consistent with previous studies of trends in climate extremes (Olmo *et al*., 2020).

When evaluating the inter-annual correspondence, most of the reanalyses presented good correlations to the linearly detrended regional average of the gridded stations reference, especially for temperature indices (Figure 6). For precipitation indices, results depended on the region and index of study, but the temporal variability was generally well represented. Nevertheless, both NCEP reanalyses exhibited much lower coefficients than the other data sets in almost all the indices. Additionally, the time series of few selected indices were shown for a better description of the temporal variability (Figure 7). Although a good agreement was generally found between data sets, CPC and the set of reanalyses tended to underestimate TXm and TXx (Figure 7a). NCEP reanalyses presented some inhomogeneities in their time series, more evident in northern Chile and the arid diagonal region of Argentina. In particular, a jump towards colder temperatures around 1998 was detected, which was probably related to the negative significant trends for temperature indices described in Figure 5. In the case of the precipitation indices (Figure 7c), reanalyses tended to overestimate R10mm and R95p in the Chilean territory and the arid diagonal region of Argentina, particularly for ERA.INTERIM. These results, in addition to the evaluation of the spatial patterns in these regions (Figure 4), evidenced ERA.INTERIM had difficulties in representing the orographic precipitation associated with the Andes mountains. In Argentinian Patagonia and southeastern South America, a greater agreement between data sets was observed, especially in the last years of the period of study, which could be associated to an increase in the quality and/or quantity of assimilated observed data.

In conclusion, the use of reanalyses data to perform regional climate studies should consider the existent differences among them and with observational data. No reanalysis was found to perform best in all the evaluated aspects, but some general remarks could be reached. The NCEP reanalyses failed in reproducing the observed trends, but presented a better performance in representing the interannual variability. The new generation of ERA reanalyses, ERA5, seemed to better reproduce the observed spatio-temporal variability than ERA.INTERIM, which was probably related to its higher spatial resolution and model improvements. It also seemed to improve the representation in complex topography areas, as it was seen for the sectors near the Andes Mountain range. In the case of JRA55, no remarkable behaviour was detected compared with the other reanalyses.

Hence, considering multiple sources of information is strongly recommended to account for observational uncertainty, especially in regions like southern South America, where data availability and its resolution are often limited. A larger network of meteorological stations with extended spatial and temporal coverage is needed to assess the quality of the information provided by reanalyses, especially in regions with few measurements such as large portions of Argentina or the highest areas of the Andes (Condom *et al*., 2020). Even more, results found in this study bring out the need to develop downscaling techniques in order to improve the misrepresentations of surface variables identified in the reanalyses, as well as to compare reanalyses performance in reproducing atmospheric circulation variables, which was probably associated to their differences found in the representation of extreme temperatures and precipitation.

Finally, this work lays the groundwork for future evaluations of the brand new global climate models in reproducing the spatio-temporal variability of temperature and precipitation in southern South America.

## ORCID

*Rocio Balmaceda-Huarte* https://orcid.org/0000-0003-2188-2797
*Matias Ezequiel Olmo* https://orcid.org/0000-0003-3324-9040
*Maria Laura Bettolli* https://orcid.org/0000-0001-7423-0544

## REFERENCES

Acharya, S.C., Nathan, R., Wang, Q.J., Su, C.H. and Eizenberg, N. (2019) An evaluation of daily precipitation from a regional

atmospheric reanalysis over Australia. *Hydrology and Earth System Sciences*, 23, 3387–3403. https://doi.org/10.5194/hess-23-3387-2019.

Bettolli, M.L., Solman, S.A., da Rocha, R.P., Llopart, M., Gutierrez, J.M., Fernández, J., Olmo, M.E., Lavín-Gullón, A., Chou, S.C., Carneiro Rodrigues, D., Coppola, E., Balmaceda Huarte, R., Barreiro, M., Blázquez, J., Doyle, M., Feijoó, M., Huth, R., Machado, L. and Vianna Cuadra, S. (2020) The CORDEX flagship pilot study in southeastern South America: a comparative study of statistical and dynamical downscaling models in simulating daily extreme precipitation events. *Climate Dynamics*. 56, 1589–1608. https://doi.org/10.1007/s00382-020-05549-z.

Burger, F., Brock, B. and Montecinos, A. (2018) Seasonal and elevational contrasts in temperature trends in Central Chile between 1979 and 2015. *Global and Planetary Change*, 162, 136–147. https://doi.org/10.1016/j.gloplacha.2018.01.005.

Cavalcanti, I.F.A. (2012) Large scale and synoptic features associated with extreme precipitation over South America: a review and case studies for the first decade of the 21st century. *Atmospheric Research*, 118, 27–40. https://doi.org/10.1016/j.atmosres.2012.06.012.

Condom, T., Martínez, R., Pabón, J.D., Costa, F., Pineda, L., Nieto, J.J., López, F. and Villacis, M. (2020) Climatological and hydrological observations for the south American Andes: in situ stations, satellite, and reanalysis data sets. *Frontiers in Earth Science*, 8, 92. https://doi.org/10.3389/feart.2020.00092.

de Barros Soares, D., Lee, H., Loikith, P.C., Barkhordarian, A. and Mechoso, C.R. (2017) Can significant trends be detected in surface air temperature and precipitation over South America in recent decades? *International Journal of Climatology*, 37, 1483–1493. https://doi.org/10.1002/joc.4792.

Dee, D.P., Uppala, S.M., Simmons, A.J., Berrisford, P., Poli, P., Kobayashi, S., Andrae, U., Balmaseda, M.A., Balsamo, G., Bauer, P., Bechtold, P., Beljaars, A.C.M., van de Berg, L., Bidlot, J., Bormann, N., Delsol, C., Dragani, R., Fuentes, M., Geer, A.J., Haimberger, L., Healy, S.B., Hersbach, H., Hólm, E. V., Isaksen, L., Kållberg, P., Köhler, M., Matricardi, M., McNally, A.P., Monge-Sanz, B.M., Morcrette, J.J., Park, B.K., Peubey, C., de Rosnay, P., Tavolato, C., Thépaut, J.N. and Vitart, F. (2011) The ERA-Interim reanalysis: configuration and performance of the data assimilation system. *Quarterly Journal of the Royal Meteorological Society*, 137, 553–597. https://doi.org/10.1002/qj.828.

Donat, M.K., Alexander, L., Herold, N. and Dittus, A. (2016) Temperature and precipitation extremes in century-long gridded observations, reanalyses, and atmospheric model simulations. *Journal of Geophysical Research – Atmospheres*, 121, 11,174–11,189. https://doi.org/10.1002/2016JD025480.

Donat, M.K., Sillman, J., Wild, S., Alexander, L., Lippmann, T. and Zwiers, F. (2014) Consistency of temperature and precipitation extremes across various global gridded in situ and reanalysis datasets. *Journal of Climate*, 27, 5019–5035. https://doi.org/10.1175/JCLI-D-13-00405.1.

du, H., Alexander, L.V., Donat, M.G., Lippmann, T., Srivastava, A., Salinger, J., Kruger, A., Choi, G., He, H.S., Fujibe, F., Rusticucci, M., Nandintsetseg, B., Manzanas, R., Rehman, S., Abbas, F., Zhai, P., Yabi, I., Stambaugh, M.C., Wang, S., Batbold, A., Oliveira, P.T., Adrees, M., Hou, W., Zong, S., Santos e Silva, C.M., Lucio, P.S. and Wu, Z. (2019) Precipitation from persistent extremes is increasing in most regions and globally. *Geophysical Research Letters*, 46, 6041–6049. https://doi.org/10.1029/2019GL081898.

Dufek, A.S., Ambrizzi, T. and da Rocha, R.P. (2008) Are reanalysis data useful for calculating climate indices over South America? *Trends and Directions in Climate Research, Annals of the New York Academy of Sciences*, 1146, 87–104.

Dulière, V., Zhang, Y. and Salathé, E. (2011) Extreme precipitation and temperature over the U.S. Pacific northwest: a comparison between observations, reanalysis data, and regional models. *Journal of Climate*, 24, 1950–1964. https://doi.org/10.1175/2010JCLI3224.1.

Espinoza, J.C., Ronchail, J., Lengaigne, M., Quispe, N., Silva, Y., Bettolli, M.L., Avalos, G. and Llacza, A. (2013) Revisiting wintertime cold air intrusions at the east of the Andes: propagating features from subtropical Argentina to Peruvian Amazon and relationship with large-scale circulation patterns. *Climate Dynamics*, 41, 1983–2002. https://doi.org/10.1007/s00382-012-1639-y.

Falco, M., Carril, A.F., Menéndez, C.G., Zaninelli, P.G. and Li, L.Z. X. (2019) Assessment of CORDEX simulations over South America: added value on seasonal climatology and resolution considerations. *Climate Dynamics*, 52, 4771–4786. https://doi.org/10.1007/s00382-018-4412-z.

Fujiwara, M., Wright, J.S., Manney, G.L., Gray, L.J., Anstey, J., Birner, T., Davis, S., Gerber, E.P., Harvey, V.L., Hegglin, M.I., Homeyer, C.R., Knox, J.A., Krüger, K., Lambert, A., Long, C.S., Martineau, P., Molod, A., Monge-Sanz, B.M., Santee, M.L., Tegtmeier, S., Chabrillat, S., Tan, D.G.H., Jackson, D.R., Polavarapu, S., Compo, G.P., Dragani, R., Ebisuzaki, W., Harada, Y., Kobayashi, C., McCarty, W., Onogi, K., Pawson, S., Simmons, A., Wargan, K., Whitaker, J.S. and Zou, C.-Z. (2017) Introduction to the SPARC reanalysis Intercomparison project (S-RIP) and overview of the reanalysis systems. *Atmospheric Chemistry and Physics*, 17, 1417–1452. https://doi.org/10.5194/acp-17-1417-2017.

Gutiérrez, J.M., Maraun, D., Widmann, M., Huth, R., Hertig, E., Benestad, R., Roessler, O., Wibig, J., Wilcke, R., Kotlarski, S., San Martín, D., Herrera, S., Bedia, J., Casanueva, A., Manzanas, R., Iturbide, M., Vrac, M., Dubrovsky, M., Ribalaygua, J., Pórtoles, J., Räty, O., Räisänen, J., Hingray, B., Raynaud, D., Casado, M.J., Ramos, P., Zerenner, T., Turco, M., Bosshard, T., Štěpánek, P., Bartholy, J., Pongracz, R., Keller, D. E., Fischer, A.M., Cardoso, R.M., Soares, P.M.M., Czernecki, B. and Pagé, C. (2019) An intercomparison of a large ensemble of statistical downscaling methods over Europe: results from the VALUE perfect predictor cross-validation experiment. *International Journal of Climatology*, 39, 3750–3785. https://doi.org/10.1002/joc.5462.

Hersbach, H. and Dee, D. (2016) ERA5 reanalysis is in production. *ECMWF Newsletter*, 147, 7.

Hoffmann, L., Günther, G., Li, D., Stein, O., Wu, X., Griessbach, S., Heng, Y., Konopka, P., Müller, R., Vogel, B. and Wright, J.S. (2019) From ERA-Interim to ERA5: the considerable impact of ECMWF's next-generation reanalysis on Lagrangian transport simulations. *Atmospheric Chemistry and Physics*, 19(5), 3097–3124.

Isotta, F., Vogel, R. and Frei, C. (2015) Evaluation of European regional reanalyses and downscalings for precipitation in the alpine region. *Meteorologische Zeitschrift*, 24, 15–37.

Iturbide, M., Bedia, J., Herrera, S., Baño-Medina, J., Fernández, J., Frías, M.D., Manzanas, R., San-Martín, D., Cimadevilla, E., Cofiño, A.S. and Gutiérrez, J.M. (2019) The R-based climate4R open framework for reproducible climate data access and post-processing. *Environmental Modelling and Software*, 111, 42–54.

Iturbide, M., Gutiérrez, J., Alves, L., Bedia, J., Cimadevilla, E., Cofiño, A., Cerezo-Mota, R., Luca, A., Faria, S., Gorodetskaya, I., Hauser, M., Herrera García, S., Hewitt, H., Hennessy, K., Jones, R., Krakovska, S., Manzanas, R., Marínez-Castro, D., Narisma, G. and Vera, C. (2020). An update of IPCC climate reference regions for subcontinental analysis of climate model data: definition and aggregated datasets. *Earth System Science Data Discussions*, 1–16. https://doi.org/10.5194/essd-2019-258

Jones, P.D., Lister, D.H., Harpham, C., Rusticucci, M. and Penalba, O. (2013) Construction of a daily precipitation grid for southeastern South America for the period 1961–2000. *International Journal of Climatology*, 33, 2508–2519. https://doi.org/10.1002/joc.3605.

Kalnay, E., Kanamitsu, M., Kistler, R., Collins, W., Deaven, D., Gandin, L., Iredell, M., Saha, S., White, G., Woollen, J., Zhu, Y., Chelliah, M., Ebisuzaki, W., Higgins, W., Janowiak, J., Mo, K. C., Ropelewski, C., Wang, J., Leetmaa, A., Reynolds, R., Jenne, R. and Joseph, D. (1996) The NCEP/NCAR 40-year reanalysis project. *Bulletin of the American Meteorological Society*, 77, 437–472.

Kanamitsu, M., Ebisuzaki, W., Woollen, J., Yang, S.K., Hnilo, J.J., Fiorino, M. and Potter, G.L. (2002) NCEP-DOE AMIP-II reanalysis (R-2). *Bulletin of the American Meteorological Society*, 83, 1631–1643.

Kendall, M.G. (1975) *Rank Correlation Methods*. London: Griffin.

Kharin, V.V., Zwiers, F.W. and Zhang, X. (2005) Intercomparison of near surface temperature and precipitation extremes in AMIP-2 simulations, reanalyses and observations. *Journal of Climate*, 18, 5201–5223.

Kistler, R., Kalnay, E., Collins, W., Saha, S., White, G., Woollen, J., Chelliah, M., Ebisuzaki, W., Kanamitsu, M., Kousky, V., van den Dool, H., Jenne, R. and Fiorino, M. (2001) The NCEP–NCAR 50-year reanalysis: monthly means CD-ROM and documentation. *Bulletin of the American Meteorological Society*, 82, 247–268. https://doi.org/10.1175/1520-0477(2001)082.

Klein Tank, A.M.G., Zwiers, F.W. and Zhang, X. (2009) Guidelines on analysis of extremes in a changing climate in support of informed decisions for adaptation. *Climate data and monitoring WCDMP*, 72, WMO-TD No. 1500, 56.

Kobayashi, S., Ota, Y., Harada, Y., Ebita, A., Moriya, M., Onoda, H., Onogi, K., Kamahori, H., Kobayashi, C., Endo, H., Miyaoka, K. and Takahashi, K. (2015) The JRA-55 reanalysis: general specifications and basic characteristics. *Journal of the Meteorological Society of Japan*, 93, 5–48. https://doi.org/10.2151/jmsj.2015-001.

Kotlarski, S., Szabó, P., Herrera, S., Räty, O., Keuler, K., Soares, P. M., Cardoso, R.M., Bosshard, T., Pagé, C., Boberg, F., Gutiérrez, J.M., Isotta, F.A., Jaczewski, A., Kreienkamp, F., Liniger, M.A., Lussana, C. and Pianko-Kluczyńska, K. (2019) Observational uncertainty and regional climate model evaluation: a pan-European perspective. *International Journal of Climatology*, 39, 3730–3749. https://doi.org/10.1002/joc.5249.

Krauskopf, T. and Huth, R. (2020) Temperature trends in Europe: comparison of different data sources. *Theoretical and Applied Climatology*, 139, 1305–1316. https://doi.org/10.1007/s00704-019-03038-w.

Lindsay, R., Wensnahan, M., Schweiger, A. and Zhang, J. (2014) Evaluation of seven different atmospheric reanalysis products in the Arctic. *Journal of Climate*, 27, 2588–2606. https://doi.org/10.1175/JCLI-D-13-00014.1.

Lovino, M.A., Müller, O.V., Berbery, E.H. and Müller, G.V. (2018) How have daily climate extremes changed in the recent past over northeastern Argentina? Elsevier science. *Global and Planetary Change*, 168(9–2018), 78–97. https://doi.org/10.1016/j.gloplacha.2018.06.008.

Luo, H., Ge, F., Yang, K., Zhu, S., Peng, T., Cai, W., Liu, X. and Tang, W. (2019) Assessment of ECMWF reanalysis data in complex terrain: can the CERA-20C and ERA-Interim data sets replicate the variation in surface air temperatures over Sichuan, China? *International Journal of Climatology*, 39, 5619–5634. https://doi.org/10.1002/joc.6175.

Mann, H.B. (1945) Nonparametric tests against trend. *Econometrica*, 13, 245–259.

Maraun, D., Wetterhall, F., Ireson, A.M., Chandler, R.E., Kendon, E.J., Widmann, M., Brienen, S., Rust, H.W., Sauter, T., Themeßl, M., Venema, V.K.C., Chun, K.P., Goodess, C.M., Jones, R.G., Onof, C., Vrac, M. and Thiele-Eich, I. (2010) Precipitation downscaling under climate change. Recent developments to bridge the gap between dynamical models and the end user. *Reviews of Geophysics*, 48(1–34), RG3003. https://doi.org/10.1029/2009RG000314.

Maraun, D. and Widmann, M. (2018) *Statistical Downscaling and Bias Correction for Climate Research*. Cambridge, UK: Cambridge University Press.

Marengo, J., Rusticucci, M., Penalba, O. and Renom, M. (2010) An intercomparison of observed and simulated extreme rainfall and temperature events during the last half of the twentieth century: part 2: historical trends. *Climatic Change*, 98 509–529. https://doi.org/10.1007/s10584-009-9743-7.

Olmo, M., Bettolli, M.L. and Rusticucci, M. (2020) Atmospheric circulation influence on temperature and precipitation individual and compound daily extreme events: spatial variability and trends over southern South America. *Weather and Climate Extremes*, 29, 100267. https://doi.org/10.1016/j.wace.2020.100267.

Parker, W.S. (2016) Reanalyses and observations. What's the difference? *Bulletin of the American Meteorological Society*, 97, 1565–1572. https://doi.org/10.1175/BAMS-D-14-00226.1.

Penalba, O.C. and Robledo, F. (2010) Spatial and temporal variability of the frequency of extreme daily rainfall regime in the La Plata Basin during the 20th century. *Climatic Change*, 98, 531–550. https://doi.org/10.1007/s10584-009-9744-6.

Penalba, O.C. and Vargas, W.M. (2004) Interdecadal and interannual variations of annual and extreme precipitation over Central-Northeastern Argentina. *International Journal of Climatology*, 24, 1565–1580. https://doi.org/10.1002/joc.1069.

Quintana, J.M. and Aceituno, P. (2012) Changes in the rainfall regime along the extratropical west coast of South America (Chile): 30-43°S. *Atmosfera*, 25, 1–12.

Re, M. and Barros, V. (2009) Extreme rainfalls in SE South America. *Climatic Change*, 96, 119–136. https://doi.org/10.1007/s10584-009-9619-x.

Rusticucci, M. and Barrucand, M. (2001) Climatología de temperaturas extremas en la Argentina. Consistencia de datos. Relación entre la temperatura media estacional y la ocurrencia de días extremos. *Meteorológica*, 26, 69–83.

Rusticucci, M. and Barrucand, M. (2004) Observed trends and changes in temperature extremes over Argentina. *Journal of Climate*, 17, 4099–4107. https://doi.org/10.1175/1520-0442.

Rusticucci, M., Barrucand, M. and Collazo, S. (2016) Temperature extremes in the Argentina central region and their monthly relationship with the mean circulation and ENSO phases. *International Journal of Climatology*, 37(6), 3003–3017. https://doi.org/10.1002/joc.4895.

Rusticucci, M. and Kousky, V. (2002) A comparative study of maximum and minimum temperatures over Argentina: NCEP/NCAR reanalysis versus station data. *Journal of Climate*, 15, 2089–2101. https://doi.org/10.1175/1520-0442(2002)015.

Rusticucci, M., Zazulie, N. and Raga, G.B. (2014) Regional winter climate of the southern Central Andes: assessing the performance of ERA-Interim for climate studies. *Journal of Geophysical Research – Atmospheres*, 119, 8568–8582. https://doi.org/10.1002/2013JD021167.

Saurral, R.I., Camilloni, I.A. and Barros, V.R. (2016) Low-frequency variability and trends in centennial precipitation stations in southern South America. *International Journal of Climatology*, 37, 4; 3-2017, 1774–1793.

Schmocker, J., Liniger, H.P., Ngeru, J.N., Brugnara, Y., Auchmann, R. and Brönnimann, S. (2016) Trends in mean and extreme precipitation in the Mount Kenya region from observations and reanalyses. *International Journal of Climatology*, 36, 1500–1514.

Schumacher, V., Justino, F., Fernández, A., Meseguer-Ruiz, O., Sarricolea, P., Comin, A., Peroni Venancio, L. and Althoff, D. (2020) Comparison between observations and gridded data sets over complex terrain in the Chilean Andes: precipitation and temperature. *International Journal of Climatology*, 40, 5266–5288. https://doi.org/10.1002/joc.6518.

Seluchi, M.E. and Marengo, J.A. (2000) Tropical–midlatitude exchange of air masses during summer and winter in South America: climatic aspects and examples of intense events. *International Journal of Climatology*, 20, 1167–1190. https://doi.org/10.1002/1097-0088(200008)20:10.

Sheridan, S.C., Lee, C.C. and Smith, E.T. (2020) A comparison between station observations and reanalysis data in the identification of extreme temperature events. *Geophysical Research Letters*, 47, e2020GL088120. https://doi.org/10.1029/2020gl088120.

Sillmann, J., Kharin, V.V., Zhang, X., Zwiers, F.W. and Bronaugh, D. (2013) Climate extremes indices in the CMIP5 multimodel ensemble: part 1. Model evaluation in the present climate. *Journal of Geophysical Research – Atmospheres*, 118, 1716–1733. https://doi.org/10.1002/jgrd.50203.

Skansi, M.M., Brunet, M., Sigró, J., Aguilar, E., Arevalo, J., Bentancur, O., Castellon, Y., Correa, R., Jácome, H., Ramos, A., Oria, C., Pasten, M., Sallons-Mitro, S., Villarroel, C., Martinez, R., Alexander, L. and Jones, P. (2013) Warming and wetting signals emerging from analysis of changes in climate extreme indices over South America. *Global and Planetary Change*, 100, 295–307. https://doi.org/10.1016/j.gloplacha.2012.11.004.

Spearman, C. (1904) The proof and measurement of association between two things. *American Journal of Psychology*, 15, 72–101.

Sterl, A. (2004) On the (in)homogeneity of reanalysis products. *Journal of Climate*, 17(19), 3866–3873.

Sun, Q., Miao, C., Duan, Q., Ashouri, H., Sorooshian, S. and Hsu, K.-L. (2018) A review of global precipitation data sets: data sources, estimation, and intercomparisons. *Reviews of Geophysics*, 56, 79–107. https://doi.org/10.1002/2017RG000574.

Taylor, K.E. (2001) Summarizing multiple aspects of model performance in a single diagram. *Journal of Geophysical Research – Atmospheres*, 106(D7), 7183–7192.

Thorne, P.W. and Vose, R.S. (2010) Reanalyses suitable for characterizing long-term trends. *Bulletin of the American Meteorological Society*, 91(3), 353–362.

Vicuña, S., Gironás, J., Meza, F.J., Cruzat, M.L., Jelinek, M., Bustos, E., Poblete, D. and Bambach, N. (2013) Exploring possible connections between hydrological extreme events and climate change in central South Chile. *Hydrological Sciences Journal*, 58(8), 1598–1619. https://doi.org/10.1080/02626667.2013.840380.

Vincent, L.A., Peterson, T.C., Barros, V.R., Marino, M.B., Rusticucci, M., Carrasco, G., Ramirez, E., Alves, L.M., Ambrizzi, T., Berlato, M.A., Grimm, A.M., Marengo, J.A., Molion, L., Moncunill, D.F., Rebello, E., Anunciação, Y.M.T., Quintana, J., Santos, J.L., Baez, J., Coronel, G., Garcia, J., Trebejo, I., Bidegain, M., Haylock, M.R. and Karoly, D. (2005) Observed trends in indices of daily temperature extremes in South America 1960–2000. *Journal of Climate*, 18, 5011–5023.

Wang, G., Zhang, X. and Zhang, S. (2019) Performance of three reanalysis precipitation datasets over the Qinling-Daba Mountains, eastern fringe of Tibetan plateau, China. *Advances in Meteorology*, 2019, 1–16. https://doi.org/10.1155/2019/7698171.

Weedon, G.P., Balsamo, G., Bellouin, N., Gomes, S., Best, M.J. and Viterbo, P. (2014) The WFDEI meteorological forcing data set: WATCH forcing data methodology applied to ERA-Interim reanalysis data. *Water Resources Research*, 50(9), 7505–7514.

Widmann, M. and Bretherton, C.S. (2000) Validation of mesoscale precipitation in the NCEP reanalysis using a new grid-cell dataset for the northwestern United States. *Journal of Climate*, 13, 1936–1950.

Wilks, D.F. (2011) *Statistical Methods in the Atmospheric Sciences*, 3rd edition. San Diego, CA: Ac. Press 627 pp.

Xie, P., Chen, M., Yang, S., Yatagai, A., Hayasaka, T., Fukushima, Y. and Liu, C. (2007) A gauge-based analysis of daily precipitation over East Asia. *Journal of Hydrometeorology*, 8, 607–626. https://doi.org/10.1175/JHM583.1.

Yang, K. and Zhang, J. (2018) Evaluation of reanalysis datasets against observational soil temperature data over China. *Climate Dynamics*, 50, 317–337. https://doi.org/10.1007/s00382-017-3610-4.

## SUPPORTING INFORMATION

Additional supporting information may be found online in the Supporting Information section at the end of this article.

**How to cite this article:** Balmaceda-Huarte R, Olmo ME, Bettolli ML, Poggi MM. Evaluation of multiple reanalyses in reproducing the spatio-temporal variability of temperature and precipitation indices over southern South America. *Int J Climatol*. 2021;1–24. https://doi.org/10.1002/joc.7142